Novel Mechanism of Foxo1 Phosphorylation in Glucagon Signaling in Control of Glucose Homeostasis

Wu, Y., Pan, Q., Yan, H., Zhang, K., Guo, X., Xu, Z., ... Guo, S. (2018). Novel Mechanism of Foxo1 Phosphorylation in Glucagon Signaling in Control of Glucose Homeostasis. Diabetes, 67(9), 1-46. DOI: 10.2337/db18-0674

Published in:
Diabetes

Document Version:
Peer reviewed version

Queen's University Belfast - Research Portal:
Link to publication record in Queen's University Belfast Research Portal

Novel Mechanism of Foxo1 Phosphorylation in Glucagon Signaling in Control of Glucose Homeostasis

Yuxin Wu[1*], Quan Pan[1*], Hui Yan[1*], Kebin Zhang[1*], Xiaoqin Guo[2, 5], Zihui Xu[1], Wanbao Yang[1], Yajuan Qi[1], Cathy A. Guo[1], Caitlyn Hornsby[1], Lin Zhang[3], Aimin Zhou[3], Ling Li[1], Yumei Chen[1], Weiping Zhang[1], Yuxiang Sun[1], Hongting Zheng[2], Fred Wondisford[5], Ling He[5], Shaodong Guo[1]

[1] Department of Nutrition and Food Science
College of Agriculture and Life Sciences
Texas A&M University
College Station, TX 77843, USA

[2] Department of Endocrinology, Third Military Medical University, Chongqing, China

[3] Departments of Chemistry,
Cleveland State University,
Cleveland, OH 02115, USA

[4] Departments of Pharmacology,
University of Texas at San Antonio, TX

[5] Division of Endocrinology, Departments of Medicine,
John Hopkins University
Baltimore, MD 04515, USA

Short running title: Foxo1 regulation by glucagon and PKA signaling

Corresponding author :
Shaodong Guo
Department of Nutrition and Food Science
College of Agriculture and Life Sciences, Texas A&M University
373 Olsen Blvd., Cater-Mattil Hall Rm. 123A, TAMU2253,
College Station, TX 77843, USA. Tel: 979-845-0850 Fax: 979-862-6842
Email: shaodong.guo@tamu.edu
* Equal contribution to the work

Diabetes Publish Ahead of Print, published online September 10, 2018

ABSTRACT

Dysregulation of hepatic glucose production (HGP) serves as a major underlying mechanism for the pathogenesis of type 2 diabetes mellitus (T2D). The pancreatic hormone glucagon increases, and insulin suppresses HGP, controlling blood glucose homeostasis. The forkhead transcription factor Foxo1 promotes HGP through increasing expression of genes encoding the rate-limiting enzymes responsible for gluconeogenesis. We previously established that insulin suppresses Foxo1 by Akt-mediated phosphorylation of Foxo1 at Ser256 in human hepatocytes. In this study, we found a novel Foxo1 regulatory mechanism by glucagon, which promotes Foxo1 nuclear translocation and stability via cAMP- and protein kinase A (PKA)-dependent phosphorylation of Foxo1 at Ser276. Replacing Foxo1-S276 with alanine (A) or aspartate (D) to block or mimic phosphorylation, respectively, markedly regulates Foxo1 stability and nuclear localization in human hepatocytes. To establish *in vivo* function of Foxo1-Ser276 phosphorylation in glucose metabolism, we generated Foxo1-S273A and Foxo1-S273D knock-in (KI) mice. The KI mice displayed impaired blood glucose homeostasis, as well as the basal and glucagon-mediated HGP in hepatocytes. Thus, Foxo1-Ser276 is a new target site identified in control of Foxo1 bioactivity and associated metabolic diseases.

INTRODUCTION

Glucagon and insulin are the most important pancreatic hormones in target tissues, such as liver, in control of glucose homeostasis in the body in response to food intake (1,2). During the fasting state, glucagon is secreted from the pancreatic α-cells to elevate blood glucose through stimulation of gluconeogenesis and glycogenolysis, protecting the body from hypoglycemia (3). However, an excess of blood glucagon level is present in animals and patients with diabetes mellitus, stimulating excessive hepatic gluconeogenesis and contributing to diabetic hyperglycemia (1,4-7).

Glucagon exerts its function through binding to the glucagon receptor (GCGR), a G-protein coupled receptor. Upon binding to glucagon, GCGR in the cell membrane activates adenylate cyclase to elevate intracellular cyclic adenosine monophosphate (cAMP) and subsequently activates PKA signaling (1,2). PKA regulates the metabolic enzymes or gene expression for glycogenolysis and gluconeogenesis, including glycogen phosphorylase, glucose-6-phosphatase catalytic subunit (G6pc), and phosphoenolpyruvate carboxykinase-1 (Pck1) (8), increasing blood glucose. Importantly, recent studies demonstrated that inhibition of GCGR by a genetic approach or chemical administration in mice significantly decreases the blood glucose and completely prevents streptozotocin (STZ)-induced hyperglycemia in type 1 diabetes mellitus (T1D) (1), suggesting that glucagon-mediated hepatic glucose production (HGP) or gluconeogenesis is a potential target for therapeutic intervention of diabetes mellitus (9,10).

Gluconeogenesis is suppressed by insulin involving in the gene transcriptional regulation in the nucleus. Foxo1, a member of the O-class of forkhead/winged helix transcription factor (Foxo), is an important component of insulin signaling cascades in regulating cellular growth, differentiation and metabolism (11). Our and other studies demonstrated that Foxo1 enhances

gene transcription of the rate-limiting enzymes responsible for gluconeogenesis, including G6pc and Pck1, through interaction with a conserved insulin-responsive element on the promoter region of the target genes (12-14), and increases HGP (11,15-17). However, insulin suppresses Foxo1 by the insulin receptor substrate1, 2 (IRS1, 2)-dependent activation of Akt that phosphorylates Foxo1 at Ser256 in human hepatocytes, which is equivalent to mouse Foxo-S253, promoting Foxo1 nuclear export and/or degradation and then decreasing HGP and blood glucose (18-21).

Foxo1 protein is stabilized in the liver of fasting mice when insulin decreases and glucagon increases in the blood circulation. Our early studies indicate that Foxo1 may partially mediate the effect of cAMP, a second messenger of glucagon, or glucocorticoid-induced expression of genes encoding gluconeogenic enzymes, such as G6pc and Pck1 (22,23). Recently, a calcium-sensing enzyme, CaMKII is shown to increase seven non-Akt phosphorylation sites of Foxo1, mediating the action of glucagon and cAMP signaling and enhancing Foxo1 nuclear localization and hepatic glucose production, but detailed phosphorylation sites involving in glucagon or cAMP signaling remain elusive *in vivo* (24). In this study, we hypothesize that Foxo1 may play a role in the action of glucagon in control of HGP or gluconeogenesis, and investigated the molecular and physiological mechanism of Foxo1 regulation by glucagon via PKA with the aim of better understanding the fundamentals of blood glucose homeostasis and pathogenesis of diabetes mellitus.

METHODS

***In vitro* kinase assay and liquid chromatography-mass spectrometry (LC-MS).** To determine whether Foxo1 is directly phosphorylated by PKA, we performed *in vitro* kinase assay, in which 20 μg of recombinant Foxo1-GST fusion protein was purchased from Millipore Inc as previously described (18). The purified Foxo1-GST recombinant protein was incubated with 5 units of recombinant PKAc (Upstate) for 1 h, at 30°C, in 50 μl reaction buffer (25 mM Tris-HCl, pH 7.0, 1 mM EGTA, 0.5 mM EDTA, 0.5 mM β-mercaptoethanol, and 3 mM magnesium acetate) with or without 0.1 mM ATP. The protein bands of interest in the SDS-PAGE gel were incised and prepared for LC-MS analysis, as described in the supplemental material.

DNA mutagenesis. Plasmid DNA expressing human Foxo1-WT was previously described (12). Oligos specific for human Foxo1-S153A, Foxo1-S153D, Foxo1-S276A, or Foxo1-S256D were designed and QuickChange™ Site-Directed Mutagenesis kit was purchased (Stratagene, La Jolla) and mutant sites were confirmed by DNA sequencing.

Mice. All animal experiments were performed according to procedures approved by Texas A&M University Institutional Animal Care and Use Committee. The floxed Foxo1 mice ($Foxo1^{L/L}$) (25), and albumin-Cre mice were previously described (26). All the mice on a C57BL/6 and 129 Sv mixed background were maintained on regular chow (Prolab Isopro 5P76). Foxo1-S273A and Foxo1-S273D knock-in (KI) mice were generated using the CRISPR/Cas9 approaches (27) and the microinjection and mouse colonies production performed by Cyagen Biosciences Inc. (Santa Clara, CA, contract number: NTMCN-150310-AML-01). The founder mice were backcrossed to C57/BL6 mice and F3 offspring male mice were used for analysis. The tail DNA of pups was genotyped by PCR and then confirmed by DNA sequencing analysis. Db/db mice were

purchased from Jackson laboratory (Bar Harbor, NM). If not specified elsewhere, all the mice were male at the ages of 8-12 weeks. For high fat diet (HFD) induced insulin resistant mouse model, 8-10 weeks old male mice were fed with HFD (42% kcal from fat, Envigo, TD.88137) or control low fat diet (LFD, 13% kcal from fat, Envigo, TD08485) for 6 months. For glucagon tolerant tests, mice after 18 h fasting were i.p. injected with glucagon of 16 μg/kg body weight and blood glucose were measured with a glucometer (Elite XL, Bayer). The dose of glucagon used was based on a recent report (28).

Generation of phosphospecific antibodies for Foxo1. We synthesized two peptides of human Foxo1 corresponding to residues 143-162 (GPLAGQPRKSpSSSRRNAWGN), and 265-285 (KSRSRAAKKKApSLQSGQEGAG), where p indicates the site of phosphorylation (S153 and S276). The peptides were conjugated to both keyhole limpet hemocyanin and bovine serum albumin and used to immunize rabbits at Covance, Denver, PA (Custom Immunology Service, CRPQ20383-01P), as previously described (18).

Blood chemistry and metabolic analysis. Serum were analyzed for insulin (Crystal Chem.) and glucagon (Alpco) using commercial protocol and reagents. Blood glucose was measured using a glucometer (Bayer). For glucagon stimulation experiments, 8 to 12-week old mice were subject an 18 h fasting and injected intraperitoneally (i.p) by glucagon (pharmaceutical grade, 0.25 mg/kg body weight) and blood glucose monitored. For GCGR antagonist injection, 6 h fasting control mice were i.v. injected with GCGR antagonist ([des-His^{1}, Glu^{9}]-glucagon amide) (1mg/kg body weight).

Protein analysis and Western-blotting. Proteins were prepared from cells or livers, resolved by SDS-PAGE and transferred to nitrocellulose membrane for immunoblotting analysis using

specific antibodies, as previously described (29). The signal intensity was measured and analyzed by NIH Image J software.

Nuclear and cytoplasmic protein extraction. Nuclear and cytoplasmic proteins from HepG2 were extracted with NE-PER nuclear (NER) and cytoplasmic (CER-I and CER-II) extraction reagent (Pierce), as previously described (29).

Gluconeogenesis, glycogenolysis, and HGP assay. The primary mouse hepatocytes were isolated from 8-12 week-old mice via 0.05% collagenase (type1, Worthington) and cultured as previously described (16). For HGP assays, freshly isolated hepatocytes were resuspended in DMEM with 2% FBS for 4 h, then rinsed with PBS, and cultured in HGP buffer (118 mM NaCl, 2.5 mM $CaCl_2$, 4.8 mM KCl, 25 mM $NaHCO_3$, 1.1 mM KH_2PO_4, 1.2 mM $MgSO_4$, 10 μM $ZnSO_4$, 0.6% BSA, 10 mM HEPES, 10 mM sodium DL-lactate, and 5 mM pyruvate, pH 7.4) in the presence or absence of 100 nM glucagon or 8-Br-cAMP. Cell culture medium was collected at 3 and 6 h, and glucose in the medium measured according to the manufacturer's protocol, using Amplex® Red Glucose_Assay (Invitrogen) (30,31). For glycogenolysis assay, lactate and pyruvate in the HGP buffer were removed and glucose release into the medium measured after treatments.

Quantitative real-time PCR. RNA was extracted with Trizol reagent (Invitrogen), cDNA synthesis used the Super-Script first-strand synthesis system (Bio-Rad), and gene expression was measured with the SYBER Green Supermix system (Bio-Rad), as previously described (29).

Gene transfection and luciferase reporter gene assay and confocal fluorescent microscope. HepG2 cells were cultured with DMEM with 10% FBS for 6 h. Cell culture were then subjected to Lipofectamine® 3000 (Life technologies) with plasmids according to manufacturer's instruction. The dual-luciferase reporter assay system from Promega was purchased and

luciferase activity measured with an Optocomp-I luminometer (MGM Instrument), and cells expressing eGFP and eGFP-Foxo1 visualized with the confocal microscope (Leica) and calculated as previously described (32).

Statistical analysis. The comparison of differences between two groups was performed using a Student's two-tailed t test to determine the significance (26). ANOVA tests were used when comparing two groups among multiple groups. All data are presented as mean± SEM. $P<0.05$ was considered statistically significant.

RESULTS

Hepatic Foxo1 is involved in glucagon-induced glucose production in mice

Previous studies from our group and others have shown that liver-specific Foxo1 knockout mice (L-F1KO) or hepatic Foxo1 suppression exhibited a 15-20% reduction in blood glucose as compared to control mice (16,17,33). To determine whether Foxo1 is involved in the action of glucagon-mediated blood glucose homeostasis, we administered glucagon intraperitoneally (i.p.) in L-F1KO and control fed-mice. Glucagon significantly increased blood glucose by 32% in control mice 60 min after glucagon injection, but the increased potential in L-F1KO mice was 21%, with a significant reduction compared to control mice (Fig. 1A). We next performed the glucagon tolerance test in the mice in the fasting state. Both control and L-F1KO mice exhibited nearly a 1.7-fold elevation in blood glucose 15 min after glucagon injection. Importantly, the ability of blood glucose increase was maintained in 60 min after glucagon injection in control mice, however L-F1KO mice exhibited a 50% reduction in blood glucose after glucagon stimulation compared with control mice ($P<0.05$, Fig. 1B). Gene expression analysis indicated that glucagon stimulated hepatic gene transcriptional levels of Igfbp-1, G6pc and Pck1 in control mice by 4.4-, 2.6-, and 2.0-fold, respectively. However, glucagon stimulation on the Igfbp-1,

G6pc, and Pck1 were 3.2-, 2.0-, and 1.8 -fold, respectively, in L-F1KO liver, exhibiting significant reductions compared to control (Fig. 1, C-E).

To determine whether Foxo1 deficiency impairs glucagon-mediated glucose production via glycogenolysis and gluconeogenesis in an autonomous manner in hepatocytes, we measured HGP with glucagon treatment in primary hepatocytes isolated from L-F1KO and control mice. Glucagon significantly increased HGP by 42 % in control hepatocytes, and by 35% in L-F1KO hepatocytes, exhibiting a 28% reduction in L-F1KO cells (Fig. 1F). Both glycogenolysis and gluconeogenesis contribute to HGP, L-F1KO cells exhibited a 50% reduction in glucagon-stimulated gluconeogenesis compared to control (46% stimulation in control vs. 23% in L-F1KO, $p<0.01$). Glucagon significantly increased glycogenolysis by 21% in control cells, L-F1KO hepatocytes had no blockage for glucagon, even though the basal level of glycogenolysis was 29% lower in L-F1KO than control cells (71 $\pm$ 4.2 μmol/h/g protein vs. 50 $\pm$ 4.9 μmol/h/g protein, $P<0.01$) (Fig. 1F). Taken together, these data indicate that Foxo1 deficiency impaired glucagon-induced liver gene expression, gluconeogenesis, and blood glucose.

Insulin and glucagon exhibit an opposite effect on Foxo1 stability in hepatocytes

We next examined the effect of insulin versus glucagon on Foxo1 regulation in hepatocytes. HepG2 cells were cultured and treated the hormones over a 6 h time course. Insulin treatment for 3 h significantly reduced total Foxo1 protein by 20%. However, glucagon treatment for 3 h significantly increased total Foxo1 protein by 1.7-fold (Fig. 2, A and B). The phosphorylation level of Foxo1 at S256 was increased 2.5-fold by insulin for 3 h treatment and persisted up to 6 h, while glucagon barely stimulated Foxo1-S256 phosphorylation even that the phosphorylation was slightly reduced at 3 h of treatment (Fig. 2, A and C). Insulin treatment for 15 min increased by 23-fold on Akt phosphorylation at T308, which was increased 5-fold by glucagon when

compared to the basal level of Akt phosphorylation in cells (Fig. 2, A and D). By contrast, insulin barely increased phosphorylation of cAMP-responsive element binding protein (CREB) at S133, a target of PKA, but glucagon treatment for 15 min significantly increased CREB-S133 phosphorylation by 1.5-fold without changing the total CREB protein level (Fig. 2, A, B and E). Moreover, Foxo1 mRNA levels were unaffected by glucagon in HepG2 cells (Fig. 2F). These results prompted us to hypothesize that glucagon may promote Foxo1 stability through activation of PKA and control Foxo1 target gene expression, impelling us to assess the impact of Foxo1 in glucagon-regulated HGP *in vivo.*

PKA stimulates and Akt inhibits the Foxo1-regulated reporter gene activity

PKA and Akt serve as important downstream effectors in glucagon and insulin signaling, respectively, in control of glucose homeostasis (15,34). In order to determine whether PKA affects Foxo1-mediated gene transcriptional activity in hepatocytes, we transfected HepG2 cells with the Igfbp-1-luciferase reporter gene construct with plasmid DNA expressing control green fluorescent protein (GFP), the catalytic subunit of PKA (PKAc), or constitutively active Akt (Myr-Akt), and then luciferase activities were measured. Overexpression of PKAc alone increased the basal promoter activity by at least 2-fold, whereas over expression of active form of Akt (MyrAkt) inhibited the promoter activity by 55% (Fig. 3A). Moreover, expression of Foxo1 alone increased Igfbp-1 promoter activity by 2.9-fold, and co-expressing PKAc and Foxo1 resulted in a robust increase of Igfbp-1 promoter activity, at least by more than 10-fold. By contrast, co-overexpression of Myr-Akt and Foxo1 almost completely diminished the Foxo1-stimulated Igfbp-1 promoter activity (Fig. 3A). Together, these data suggest that PKA had an additive effect on promoting Foxo1-stimulated Igfbp-1 promoter activity.

Identification of novel serine/threonine phosphorylation sites of Foxo1 by PKA

Analysis of Foxo1 phosphorylation sites (http://scansite.mit.edu) revealed that human Foxo1 contains three PKA consensus sequences (R/KXRT/S, R-Arginine, K-Lysine, X-any amino acid), located at Ser153, Thr182, and Ser276, which are evolutionarily conserved across species (Fig. 3B). We hypothesize that glucagon-activated PKA phosphorylates Foxo1 via these putative PKA phosphorylation sites and enhances Foxo1 stability and transcriptional activity.

Next, we performed *in vitro* kinase assay to determine whether PKA can directly phosphorylate Foxo1. Glutathione-S-transferase-fused Foxo1 (Foxo1-GST) and active PKA catalytic subunit were incubated in a protein kinase assay buffer system and then resolved by SDS-PAGE followed by the Coomassie-brilliant blue staining. Phosphorylated Foxo1 fragment (60 kDa) by PKAc slightly upshifted in mobility (Fig. 3C). The Foxo1-GST protein (105 kDa) and Foxo1 fragment (60 kDa) were incised from the gel and subjected to LC-MS/MS analyses. The results from Mascot analysis of mass spectrometry (MS) of PKAc with/without ATP-treated samples indicated a presence and high score for Foxo1-S276 phosphorylation, a low score for Foxo1-S153 phosphorylation, and no presence and score for T182 phosphorylation (Fig. 3D). Based on these results, we generated the phosphospecific antibody against human Foxo1-S276 or Foxo1-S153, which is equivalent to mouse Foxo1-S273 or S150, respectively. In HepG2 cells, glucagon significantly stimulated the phosphorylation of Foxo1-S273 and S153 by 2.5-fold and 1.5-fold, respectively (Fig. 3E). The phosphorylation of S276 and S153 by glucagon was blocked when PKA catalytic subunit C (PKACB) was knockdown by siRNA(Fig. 3E). The knockdown of PKA markedly decreased glucagon-stimulated CREB phosphorylation and Foxo1 protein level, suggesting that PKA is essential for maintaining Foxo1 protein stability (Fig. 3E). We further confirmed these findings in mouse primary hepatocytes, glucagon treatment enhanced the phosphorylation of Foxo1 at S273 and S150, as well as total Foxo1 protein levels, while these

effects of glucagon were abolished in the cells when treated with H89, a PKA chemical inhibitor (Fig. 3F). In mouse liver, glucagon injection resulted in a 3.8-fold increase in Foxo1-S273 phosphorylation and a 1.6-fold increase in Foxo1-S150 phosphorylation (Fig. 4A). Moreover, we administered GCGR antagonist into WT mice and examined whether endogenous Foxo1 protein level is regulated by the glucagon receptor in the liver. Intravenous injection of GCGR antagonist ([des-His^{1}, Glu^{9}]-Glucagon amide) resulted in a 20% decrease in blood glucose (Fig. 4, B and C), as well as a 60% decrease of CREB phosphorylation, 55% decrease in Foxo1-S273 phosphorylation, and 35% decrease in total Foxo1 protein level, while Foxo1-S150 phosphorylation was barely affected compared to vehicle treatment (Fig. 4D). These results suggest that glucagon signaling via its receptor and PKA stimulates hepatic Foxo1 phosphorylation at S273, enhancing Foxo1 stability.

Human Foxo1-S276 phosphorylation promotes Foxo1 nuclear localization

We next examined whether the newly identified Foxo1 phosphorylation sites play a role in Foxo1 nuclear/cytoplasmic trafficking and stability in cells. We generated plasmid DNA expressing GFP-Foxo1-WT (wild-type), GFP-Foxo1-S153A, or GFP-Foxo1-S276A, in which serine residue was substituted with an alanine (A) at S153 or S276 to block phosphorylation, whereas GFP-Foxo1-S153D or GFP-Foxo1-S276D containing an aspartate (D) substitution to mimic phosphorylation by introduction of a negative charge. HepG2 cells were transfected with one of these plasmids and then stimulated with 8-Br-cAMP for 15 min prior to confocal imaging. In cells that overexpressed Foxo1-WT, Foxo1 localized in both cytoplasm and nucleus at the basal level, but cAMP stimulation promoted Foxo1 nuclear localization. However, cAMP-induced Foxo1-nuclear localization was blocked by S276A mutation, in which overexpressed Foxo1-S276A dispersed primarily within the cytoplasm. Conversely, Foxo1-S276D primarily

localized in the nucleus (Fig. 5). Compared to Foxo1-WT, Foxo1-S153A or S153D did not exhibit distinct differences in Foxo1 subcellular localization in cells, and overexpressed Foxo1-S153A and 153D were primarily located to the nucleus in responses to cAMP, similar to Foxo1-WT (Fig. 5). Thus, these results suggest that Foxo1-S276 phosphorylation is crucial for mediating cAMP-stimulated Foxo1 nuclear localization.

To confirm the Foxo1 subcellular localization upon glucagon or cAMP stimulation, we extracted nuclear and cytoplasmic protein from cells for Foxo1 analysis. Glucagon or cAMP stimulated endogenous Foxo1 nuclear localization by nearly 3-fold compared to vehicle control group (Fig. 6A, $P<0.05$). By contrast, insulin reduced nuclear total Foxo1 by 25% (Fig. 6A). These data indicate that either glucagon or cAMP induced Foxo1 nuclear localization, which is distinct from insulin.

Foxo1-S276 phosphorylation enhances Foxo1 stability in cells

We next further focused on Foxo1-S276 phosphorylation in control of Foxo1 stability in cells. HepG2 cells were transfected with plasmid DNA that expresses Foxo1-WT, Foxo1-S276A, or Foxo1-S276D and then stimulated with glucagon for 30 min followed by nuclear and cytoplasmic protein extraction. In Foxo1-WT transfected cells, glucagon increased total Foxo1 protein in the nucleus by 1.5-fold (Fig. 6, B and C). Importantly, Foxo1-S276D protein, which mimics S276 phosphorylation with introduction of a negative charge, increased total Foxo1 protein abundance in both nucleus and cytoplasm, mimicking the effect of glucagon on Foxo1 nuclear localization (Fig. 6, B). By contrast, Foxo1-S276A, which contains a substitution of alanine, largely prevented glucagon-stimulated Foxo1 nuclear localization (Fig. 6C).

To further examine the mechanism of Foxo1-S276 phosphorylation in control of Foxo1 stability, we transfected with an equal amount of Foxo1 gene construct with HepG2 cells and

then treated cells for 8 h with MG132, a 26S proteasome complex inhibitor, preventing Foxo1 protein ubiquitination or cycloheximide (CHX), a protein synthesis inhibitor, inhibiting Foxo1 protein synthesis. When Foxo1-WT, Foxo1-S276A, or Foxo1-S276D plasmid DNA was transfected, the total Foxo1 protein in Foxo1-S276A group was reduced by 50% compared to overexpressed Foxo1-WT ($P<0.05$, Fig. 6D). However, in the MG132-treated group, the reduction of Foxo1-S276A protein was totally prevented and Foxo1-S276A protein was restored and stabilized to a normal level when compared to Foxo1-WT, and there was no significant difference in total Foxo1 protein levels observed in all the cells transfected with Foxo1-WT, S276A, or S276D (Fig. 6D). Moreover, when Foxo1 protein synthesis inhibited by CHX in cells, the remaining Foxo1 protein level in Foxo1-S276D group increased by 40%, while decreased by 44% in Foxo1-S276A group compared to Foxo1-WT group (Fig. 6D). These data suggest that Foxo1-S276 phosphorylation promoted Foxo1 stability, while non-phosphorylation of S276 enhanced 26S proteasome-dependent degradation of Foxo1.

Foxo1-S276 phosphorylation impairs insulin-induced Foxo1 ubiquitination and Foxo1 nuclear export

We next determined whether Foxo1-S276 phosphorylation or Foxo1-S276D affects insulin-induced Foxo1 ubiquitination in cells. HepG2 cells were transfected with equal amount of Foxo1-WT or S276D plasmid DNA together with ubiquitin for 10 h and then stimulated with insulin for additional 12 h, total cellular proteins were extracted for analysis. Western-blotting analysis revealed that insulin reduced total Foxo1 protein by 50% in Foxo1-WT or S276A expressed cells, while the effect of insulin was abolished in cells expressing Foxo1-S276D mutant (Fig. 6E).

We further assessed whether Foxo1-S276 phosphorylation or Foxo1-S276D affects insulin-induced Foxo1 nuclear translocation in cells. HepG2 cells were transfected with equal amount of Foxo1-WT or S276D plasmid DNA for 18 h and then stimulated with insulin over a 120-min time course. Upon insulin stimulation for either 90 min or 120 min, Foxo1-WT protein was primarily located in the cytoplasm (Fig. 7, A-C). Foxo1-S276D protein primarily localized at both cytoplasm and nucleus with increased levels compared to Foxo1-WT. However, Foxo1-S276D largely blocked insulin-stimulated nuclear export, particularly at 120 min treatment of insulin (Fig. 7A), which was confirmed by Western-blotting. Moreover, the blotting result showed that the cytoplasmic Foxo1-S256 phosphorylation by insulin for 90 or 120 min treatment was significantly impaired by S276D mutation since the basal level of Foxo1-S256 phosphorylation was higher in S276D than WT in cells (Fig. 7, B and C). These results reveal that Foxo1-S276 phosphorylation or aspartate mutation promoted Foxo1 nuclear localization and stability and impaired the ability of insulin to induce Foxo1 nuclear export and/or degradation, which may serve as a mechanism for insulin resistance at the Foxo1 level.

Foxo1-S273 phosphorylation controls blood glucose homeostasis and hepatic glucose production in mice

To further explore the physiological function of equivalent human Foxo1-S276 in glucose metabolism in mice, we used the CRISPR/Cas9 approach to generate Foxo1-S273A and Foxo1-S273D knock-in mice, where the endogenous Foxo1-S273 alleles were replaced by alanine (A) mutations or aspartate (D) mutations (Fig. S1). All the mice survived with no obvious physiological deficiency. The feeding blood glucose increased by 20% in Foxo1-S276$^{D/D}$ mice and there was no change in Foxo1-S276$^{A/A}$ mice compared to control. The fasting blood glucose increased by 31% in Foxo1-S276$^{D/D}$ mice but decreased significantly by 10% in Foxo1-S276$^{A/A}$

mice (Fig. 8A). Hepatic Igfbp-1 and G6pc mRNA expression significantly increased by 4.5- and 2.1-fold in the liver of Foxo1-S273$^{D/D}$ compared to control liver, respectively. However, there was a 25% reduction for both gene expression in S273$^{A/A}$ liver compared to control liver ($P<0.05$, Fig. 8B). The total Foxo1 protein level in the liver was increased by 2.6-fold in Foxo1-S273$^{D/D}$ mice, but reduced by 40% in Foxo1-S273$^{A/A}$ mice when compared to control ($P<0.05$, Fig. 8C).

We further assessed the direct role of Foxo1-S273 phosphorylation in control of HGP, using the primary hepatocytes isolated from Foxo1-S273$^{A/A}$, S273$^{D/D}$, and WT mice. The basal level of HGP was increased by 46% in Foxo1-S273$^{D/D}$ hepatocytes, but the basal potential was reduced by 40% in Foxo1-S273$^{A/A}$ hepatocytes, compared to control hepatocytes ($P<0.01$, Fig. 8D). Upon glucagon stimulation, HGP was increased by 53% in control hepatocytes; however, this stimulatory effect was significantly impaired or attenuated by either Foxo1-S273D or S273A mutation, which exhibited an increase by 41% or 20%, respectively ($P<0.01$, Fig. 8D). Glucagon-stimulated glycogenolysis barely impaired by Foxo1 mutation in the cells.

We next performed glucagon tolerance tests in Foxo1-S273$^{A/A}$, S273$^{D/D}$, and WT mice in the fasting state. Both WT and Foxo1-S273$^{D/D}$ mice exhibited a 1.8-fold increase and Foxo1-S273$^{A/A}$ mice had a 1.6-fold increase in blood glucose after 15 min of glucagon injection, indicating that Foxo1-S273$^{A/A}$ mutant impaired glucagon stimulation of blood glucose. Importantly, in WT and Foxo1-S273$^{A/A}$ mice, blood glucose returned to initial level 60 min after glucagon injection, however, high blood glucose level was maintained in Foxo1-S273$^{D/D}$ mice, indicating that Foxo1-S273$^{D/D}$ mutant prolonged glucagon stimulation of blood glucose ($P<0.05$, Fig. 8 E and F). The impaired effects of glucagon stimulation on HGP and blood glucose by Foxo1 mutations at S273 suggest an important role of Foxo1-S273 phosphorylation plays in glucagon signaling in control of hepatic gluconeogenesis and blood glucose.

Foxo1-S273 phosphorylation increases in the liver of db/db and HFD-fed mice

Finally, we examined Foxo1-S273 phosphorylation in the liver of db/db diabetic mice, as well as HFD-induced insulin resistantmice. The db/db mice exhibited elevations in blood glucagon, glucose, and serum insulin by 3-fold, 3-fold, and 10-fold, respectively, compared to control mice (Fig. 8G). Moreover, total Foxo1 protein and S273 phosphorylation significantly increased in the liver of db/db mice and accumulated in the nucleus (Fig. 8H). In parallel with increased Foxo1-S273 phosphorylation and PKA-T197 phosphorylation indicative of PKA activity, also markedly enhanced in both nucleus and cytoplasm in the liver of db/db mice (Fig. 8I). The HFD-fed mice exhibited increased blood glucagon, glucose and serum insulin by 1.8-, 1.4-, and 5-fold, respectively, compared to LFD-fed mice (Figure 8J). Moreover, total Foxo1 protein and Foxo1-S273 phosphorylation significantly increased in liver of HFD-fed mice when compared to the LFD-fed liver (Fig.8, K andL). These data suggest that Foxo1-S273 phosphorylation and its nuclear retention, along with excess glucagon and PKA activity, coexist in the liver of animals with T2D or insulin resistance.

DISCUSSION

We and other groups have previously established that insulin phosphorylates human Foxo1-S256 by activation of Akt that promotes Foxo1 cytoplasmic sequestration or nuclear export, and then suppresses expression of genes responsible for HGP (12,18,20,21,35). In this study, using *in vitro* kinase assay-coupled LC/MS, phosphospecific antibodies, and CRISPR/Cas9–based Foxo1 KI mutant mice, we were able to identify a novel molecular, cellular and physiological mechanism by which Foxo1 mediates glucagon signaling via phosphorylation at Ser276 (human) or Ser273 (mouse) in control of hepatic gluconeogenesis and blood glucose.

Glucagon has been implicated in the pathogenesis of diabetic hyperglycemia, largely by enhancing HGP, which is believed to be a key mechanism for pathogenesis of diabetes mellitus (36). In mice with T2D, we recently demonstrated that hepatic Foxo1 deletion reduced HGP and blood glucose in db/db mice (16). Given that a high glucagon level is present in both types of diabetes (6), hyper-activation of Foxo1 by activated PKA and inactivated Akt upon insulin resistance or deficiency may serve as a fundamental mechanism for excess liver gluconeogenesis resulting in diabetic hyperglycemia.

The mechanism by which Foxo1-S276 phosphorylation promotes Foxo1 nuclear retention and stability is involved in the prevention of proteasome-mediated Foxo1 ubiquitination. We expect that Foxo1-S276 phosphorylation might enhance its recruitment with a number of co-factors, such as importin or CREB, to participate in Foxo1 subcellular trafficking and gene transcription, but detailed molecular aspects warrant further investigation. By activating heterologous signaling cascades, glucagon primarily activates PKA and downstream effectors,

including glycogen phosphorylase for glycogenolysis and CREB for gluconeogenesis (9,37). Glucagon also minimally activates Akt phosphorylation, but its duration and intensity seemed insufficient for induction of Foxo1-S256 phosphorylation and degradation (Fig. 2). Thus, insulin is a major hormone for the endogenous Akt activation downstream of the IRS1, 2-associated PI3K, as we observed in the liver or heart of male mice (15,26,38). In this study, our *in vitro* data established that Foxo1-S276 is a target of PKA in glucagon signaling and promotes Foxo1 nuclear retention. Foxo1-S276D mutation mimics Foxo1-S276 phosphorylation and promotes Foxo1 nuclear localization and stability. Moreover, Foxo1-S273D mutation impairs the ability of insulin-stimulated Foxo1 nuclear export or cytoplasmic sequestration. This finding suggests a novel mechanism for insulin resistance when Foxo1-S273 phosphorylated. Conversely, Foxo1-S276A mutation, which blocks phosphorylation, enhances Foxo1 ubiquitination and/or degradation, a process reversed by the 28S proteasome inhibitor MG132. This study reveals a unique mechanism of Foxo1 regulation by which glucagon stimulates HGP via Foxo1 at the post-translational level.

Foxo1 can be regulated by multiple protein kinases (15). It has been shown that mitogen-activated protein kinase (MAPK) phosphorylates Foxo1 at S246, S284, S295, S326, S413, S415, S429, S467, S475 and T557, and p38α phosphorylates five of the ten sites-S284, S295, S326, S467 and S475 (39). Moreover, these phosphorylation sites are shared by CaMKII, and expression of a Foxo1-S7A mutation (S246A/S284A/S295A/S413A/S415A/S429A/S475A) attenuated glucagon-induced Foxo1 nuclear localization, and it is suggested that CaMKII promotes Foxo1 nuclear localization through p38α activation that stimulates hepatic gluconeogenesis (24,40). The Foxo1-S273 phosphorylation identified as a target of PKA is distinct from these sites, but whether it is involved by other protein kinases, such as p38α, remain to be determined.

HGP is generally regulated by direct mechanisms of insulin action in hepatocytes autonomously (41). Our early studies suggest that direct hepatocytes signaling via IRS1, 2-mediated Akt activation or hepatic Foxo1 suppression is required for hepatic insulin suppression on HGP and blood glucose (26). However, a recent report suggests that an indirect insulin that suppresses free fatty acid influx to hepatocytes from lipolysis of adipose tissue is critical for suppression of HGP so that hepatocyte Akt signaling is dispensable for HGP suppression (42). Indeed, HGP can be regulated by indirect insulin action in extrahepatic tissues non-autonomously (41). In addition to suppress glucagon secretion from pancreatic α-cells or antagonize the effect of cAMP , insulin also suppresses HGP by the central nervous system (CNS) in hypothalamic neurons via a vagal efferent (43). Thus, we do not rule out the possibility of other tissues including CNS, adipose tissue, and pancreas on HGP control in the L-F1KO and KI mouse models, but our data from mouse primary hepatocytes do support that the cellular autonomous effect of glucagon in hepatocytes has critical roles in controlling Foxo1, gluconeogenesis, and HGP.

Foxo1 has a variety of target genes responsible for multiple physiological functions in the body (11,15,44,45). We have recently identified other two Foxo1 target genes in the liver, such as angiotensinogen, a precursor of angiotensin II (AngII) that regulates blood pressure (44). Foxo1 also promotes expression of heme oxygenase-1 (HO-1), reducing synthesis of heme and mitochondria (46) and driving bodily metabolic inflammation and insulin resistance in mice and humans (47). In this study, we demonstrated a novel regulatory mechanism of Foxo1 by glucagon-cAMP-PKA signaling in hepatocytes, but we do not rule out the possibility of a similar Foxo1 regulation by other hormones via activation of PKA in tissues, including but not limited to glucagon (48). Indeed, hormones such as catecholamines or glucocorticoids also increases

hepatic gluconeogenesis or promote insulin resistance under certain conditions involving activation of PKA, such as stress (49). Our studies demonstrate that Foxo1 is a mediator of multiple signaling cascades, e.g. PKA and Akt; it integrates different hormones and intracellular protein kinases into the nuclear gene transcriptional programming in control of insulin sensitivity, HGP, blood glucose. Thus, Foxo1-S276 phosphorylation may not only serve as a novel and important biomarker for Foxo1 stability and bioactivity contributing to hyperglycemia upon development of diabetes mellitus, but also provide a potential therapeutic target in control of Foxo1 stability and activity to prevent diabetes mellitus and associated diseases in the future.

AUTHOR CONTRIBUTIONS

S.G. conceived of the hypothesis and designed the experiments.

Y. W., Q. P., K. Z., H. Y., X. G., Z. X., W. Y.,Y. Q., C. G., C. H., L. Z., A. Z., L. L., and Y. C. performed experiments. W. Z., Y. S., H. Z., F. W., and L. H. analyzed and interpreted data. L.Z. and A.Z. performed LC/MS and analyzed the data. Y. W., Q. P., H. Y., and S. G. wrote the manuscript.

ACKNOWLEDGMENTS

This study was supported by grants from the National Institutes of Health (RO1 DK095118), American Diabetes Association Career Development Award (1-15-CD-09) and Minority Undergraduate Internship Award (1-17-MUI-008), the American Heart Association (BGIA-7880040), Faculty Start-up from the Texas A&M University Health Science Center and AgriLife Research, and the USDA National Institute of Food and Agriculture (Hatch 1010958) to S.G. Dr. S. Guo is recipient of the year 2015 American Diabetes Association Research Excellence Thomas R. Lee Award. We thank Mr. Mike Honig who provided English editing for the manuscript. S. G. also would like to thank the scientists at Covance (Denvor, USA) and Cyagen Biosciences (Santa Clara, USA) for help generating Foxo1 phosphospecific antibodies and KI mice, respectively. S.G. is the guarantor of this work and as such, had full access to all the data in the study and takes responsibility for the integrity of the data and accuracy of the data analysis.

COMPETING INTERESTS STATEMENT

The authors declare that they have no competing financial interest.

REFERENCES

1.Ali, S., and Drucker, D. J. (2009) Benefits and limitations of reducing glucagon action for the treatment of type 2 diabetes. *Am J Physiol Endocrinol Metab* **296**, E415-421

2.Edgerton, D. S., and Cherrington, A. D. (2011) Glucagon as a critical factor in the pathology of diabetes. *Diabetes* **60**, 377-380

3.Unger, R. H. (1971) Glucagon physiology and pathophysiology. *N Engl J Med* **285**, 443-449

4.Tahrani, A. A., Bailey, C. J., Del Prato, S., and Barnett, A. H. (2011) Management of type 2 diabetes: new and future developments in treatment. *Lancet* **378**, 182-197

5.Johnson, D. G., Goebel, C. U., Hruby, V. J., Bregman, M. D., and Trivedi, D. (1982) Hyperglycemia of diabetic rats decreased by a glucagon receptor antagonist. *Science* **215**, 1115-1116

6.Lee, Y., Wang, M. Y., Du, X. Q., Charron, M. J., and Unger, R. H. (2011) Glucagon receptor knockout prevents insulin-deficient type 1 diabetes in mice. *Diabetes* **60**, 391-397

7.Lund, A., Bagger, J. I., Wewer Albrechtsen, N. J., Christensen, M., Grondahl, M., Hartmann, B., Mathiesen, E. R., Hansen, C. P., Storkholm, J. H., van Hall, G., Rehfeld, J. F., Hornburg, D., Meissner, F., Mann, M., Larsen, S., Holst, J. J., Vilsboll, T., and Knop, F. K. (2016) Evidence of Extrapancreatic Glucagon Secretion in Man. *Diabetes* **65**, 585-597

8.Mayr, B., and Montminy, M. (2001) Transcriptional regulation by the phosphorylation-dependent factor CREB. *Nat Rev Mol Cell Biol* **2**, 599-609

9.An, H., and He, L. (2016) Current understanding of metformin effect on the control of hyperglycemia in diabetes. *J Endocrinol* **228**, R97-106

10.He, L., Sabet, A., Djedjos, S., Miller, R., Sun, X., Hussain, M. A., Radovick, S., and Wondisford, F. E. (2009) Metformin and insulin suppress hepatic gluconeogenesis through phosphorylation of CREB binding protein. *Cell* **137**, 635-646

11.Accili, D., and Arden, K. C. (2004) FoxOs at the crossroads of cellular metabolism, differentiation, and transformation. *Cell* **117**, 421-426

12.Guo, S., Rena, G., Cichy, S., He, X., Cohen, P., and Unterman, T. (1999) Phosphorylation of serine 256 by protein kinase B disrupts transactivation by FKHR and mediates effects of insulin on insulin-like growth factor-binding protein-1 promoter activity through a conserved insulin response sequence. *J Biol Chem* **274**, 17184-17192

13.O'Brien, R. M., Lucas, P. C., Forest, C. D., Magnuson, M. A., and Granner, D. K. (1990) Identification of a sequence in the PEPCK gene that mediates a negative effect of insulin on transcription. *Science* **249**, 533-537

14.Onuma, H., Vander Kooi, B. T., Boustead, J. N., Oeser, J. K., and O'Brien, R. M. (2006) Correlation between FOXO1a (FKHR) and FOXO3a (FKHRL1) binding and the

inhibition of basal glucose-6-phosphatase catalytic subunit gene transcription by insulin. *Mol Endocrinol* **20**, 2831-2847

15.Guo, S. (2014) Insulin signaling, resistance, and the metabolic syndrome: insights from mouse models into disease mechanisms. *J Endocrinol* **220**, T1-T23

16.Zhang, K., Li, L., Qi, Y., Zhu, X., Gan, B., DePinho, R. A., Averitt, T., and Guo, S. (2012) Hepatic suppression of Foxo1 and Foxo3 causes hypoglycemia and hyperlipidemia in mice. *Endocrinology* **153**, 631-646

17.Altomonte, J., Richter, A., Harbaran, S., Suriawinata, J., Nakae, J., Thung, S. N., Meseck, M., Accili, D., and Dong, H. (2003) Inhibition of Foxo1 function is associated with improved fasting glycemia in diabetic mice. *Am J Physiol Endocrinol Metab* **285**, E718-728

18.Rena, G., Guo, S., Cichy, S. C., Unterman, T. G., and Cohen, P. (1999) Phosphorylation of the transcription factor forkhead family member FKHR by protein kinase B. *J Biol Chem* **274**, 17179-17183

19.Dong, X. C., Copps, K. D., Guo, S., Li, Y., Kollipara, R., DePinho, R. A., and White, M. F. (2008) Inactivation of hepatic Foxo1 by insulin signaling is required for adaptive nutrient homeostasis and endocrine growth regulation. *Cell Metab* **8**, 65-76

20.Nakae, J., Park, B. C., and Accili, D. (1999) Insulin stimulates phosphorylation of the forkhead transcription factor FKHR on serine 253 through a Wortmannin-sensitive pathway. *J Biol Chem* **274**, 15982-15985

21.Biggs, W. H., 3rd, Meisenhelder, J., Hunter, T., Cavenee, W. K., and Arden, K. C. (1999) Protein kinase B/Akt-mediated phosphorylation promotes nuclear exclusion of the winged helix transcription factor FKHR1. *Proc Natl Acad Sci U S A* **96**, 7421-7426

22.Schmoll, D., Walker, K. S., Alessi, D. R., Grempler, R., Burchell, A., Guo, S., Walther, R., and Unterman, T. G. (2000) Regulation of glucose-6-phosphatase gene expression by protein kinase Balpha and the forkhead transcription factor FKHR. Evidence for insulin response unit-dependent and -independent effects of insulin on promoter activity. *J Biol Chem* **275**, 36324-36333

23.Yeagley, D., Guo, S., Unterman, T., and Quinn, P. G. (2001) Gene- and activation-specific mechanisms for insulin inhibition of basal and glucocorticoid-induced insulin-like growth factor binding protein-1 and phosphoenolpyruvate carboxykinase transcription. Roles of forkhead and insulin response sequences. *J Biol Chem* **276**, 33705-33710

24.Ozcan, L., Wong, C. C., Li, G., Xu, T., Pajvani, U., Park, S. K., Wronska, A., Chen, B. X., Marks, A. R., Fukamizu, A., Backs, J., Singer, H. A., Yates, J. R., 3rd, Accili, D., and Tabas, I. (2012) Calcium signaling through CaMKII regulates hepatic glucose production in fasting and obesity. *Cell Metab* **15**, 739-751

25.Paik, J. H., Kollipara, R., Chu, G., Ji, H., Xiao, Y., Ding, Z., Miao, L., Tothova, Z., Horner, J. W., Carrasco, D. R., Jiang, S., Gilliland, D. G., Chin, L., Wong, W. H., Castrillon, D. H., and DePinho, R. A. (2007) FoxOs are lineage-restricted redundant tumor suppressors and regulate endothelial cell homeostasis. *Cell* **128**, 309-323

26.Guo, S., Copps, K. D., Dong, X., Park, S., Cheng, Z., Pocai, A., Rossetti, L., Sajan, M., Farese, R. V., and White, M. F. (2009) The Irs1 branch of the insulin signaling cascade plays a dominant role in hepatic nutrient homeostasis. *Mol Cell Biol* **29**, 5070-5083

27.Wang, H., Yang, H., Shivalila, C. S., Dawlaty, M. M., Cheng, A. W., Zhang, F., and Jaenisch, R. (2013) One-step generation of mice carrying mutations in multiple genes by CRISPR/Cas-mediated genome engineering. *Cell* **153**, 910-918

28.Rossi, M., Zhu, L., McMillin, S. M., Pydi, S. P., Jain, S., Wang, L., Cui, Y., Lee, R. J., Cohen, A. H., Kaneto, H., Birnbaum, M. J., Ma, Y., Rotman, Y., Liu, J., Cyphert, T. J., Finkel, T., McGuinness, O. P., and Wess, J. (2018) Hepatic Gi signaling regulates whole-body glucose homeostasis. *J Clin Invest* **128**, 746-759

29.Guo, S., Dunn, S. L., and White, M. F. (2006) The reciprocal stability of FOXO1 and IRS2 creates a regulatory circuit that controls insulin signaling. *Mol Endocrinol* **20**, 3389-3399

30.Chen, Z., Sheng, L., Shen, H., Zhao, Y., Wang, S., Brink, R., and Rui, L. (2012) Hepatic TRAF2 regulates glucose metabolism through enhancing glucagon responses. *Diabetes* **61**, 566-573

31.Sun, Z., Miller, R. A., Patel, R. T., Chen, J., Dhir, R., Wang, H., Zhang, D., Graham, M. J., Unterman, T. G., Shulman, G. I., Sztalryd, C., Bennett, M. J., Ahima, R. S., Birnbaum, M. J., and Lazar, M. A. (2012) Hepatic Hdac3 promotes gluconeogenesis by repressing lipid synthesis and sequestration. *Nat Med* **18**, 934-942

32.Zhang, X., Gan, L., Pan, H., Guo, S., He, X., Olson, S. T., Mesecar, A., Adam, S., and Unterman, T. G. (2002) Phosphorylation of serine 256 suppresses transactivation by FKHR (FOXO1) by multiple mechanisms. Direct and indirect effects on nuclear/cytoplasmic shuttling and DNA binding. *J Biol Chem* **277**, 45276-45284

33.Matsumoto, M., Pocai, A., Rossetti, L., Depinho, R. A., and Accili, D. (2007) Impaired regulation of hepatic glucose production in mice lacking the forkhead transcription factor Foxo1 in liver. *Cell Metab* **6**, 208-216

34.Gromada, J., Duttaroy, A., and Rorsman, P. (2009) The insulin receptor talks to glucagon? *Cell Metab* **9**, 303-305

35.Huang, H., Regan, K. M., Wang, F., Wang, D., Smith, D. I., van Deursen, J. M., and Tindall, D. J. (2005) Skp2 inhibits FOXO1 in tumor suppression through ubiquitin-mediated degradation. *Proc Natl Acad Sci U S A* **102**, 1649-1654

36.Unger, R. H., and Cherrington, A. D. (2012) Glucagonocentric restructuring of diabetes: a pathophysiologic and therapeutic makeover. *J Clin Invest* **122**, 4-12

37.Altarejos, J. Y., and Montminy, M. (2011) CREB and the CRTC co-activators: sensors for hormonal and metabolic signals. *Nat Rev Mol Cell Biol* **12**, 141-151

38.Qi, Y., Xu, Z., Zhu, Q., Thomas, C., Kumar, R., Feng, H., Dostal, D. E., White, M. F., Baker, K. M., and Guo, S. (2013) Myocardial Loss of IRS1 and IRS2 Causes Heart Failure and Is Controlled by p38alpha MAPK During Insulin Resistance. *Diabetes* **62**, 3887-3900

39.Asada, S., Daitoku, H., Matsuzaki, H., Saito, T., Sudo, T., Mukai, H., Iwashita, S., Kako, K., Kishi, T., Kasuya, Y., and Fukamizu, A. (2007) Mitogen-activated protein kinases, Erk and p38, phosphorylate and regulate Foxo1. *Cell Signal* **19**, 519-527

40.Cao, W., Collins, Q. F., Becker, T. C., Robidoux, J., Lupo, E. G., Jr., Xiong, Y., Daniel, K. W., Floering, L., and Collins, S. (2005) p38 Mitogen-activated protein kinase plays a stimulatory role in hepatic gluconeogenesis. *J Biol Chem* **280**, 42731-42737

41.Cherrington, A. D., Edgerton, D., and Sindelar, D. K. (1998) The direct and indirect effects of insulin on hepatic glucose production in vivo. *Diabetologia* **41**, 987-996

42.Titchenell, P. M., Quinn, W. J., Lu, M., Chu, Q., Lu, W., Li, C., Chen, H., Monks, B. R., Chen, J., Rabinowitz, J. D., and Birnbaum, M. J. (2016) Direct Hepatocyte Insulin Signaling Is Required for Lipogenesis but Is Dispensable for the Suppression of Glucose Production. *Cell Metab* **23**, 1154-1166

43.Myers, M. G., Jr., and Olson, D. P. (2012) Central nervous system control of metabolism. *Nature* **491**, 357-363

44.Qi, Y., Zhang, K., Wu, Y., Xu, Z., Yong, Q. C., Kumar, R., Baker, K. M., Zhu, Q., Chen, S., and Guo, S. (2014) Novel mechanism of blood pressure regulation by forkhead box class O1-mediated transcriptional control of hepatic angiotensinogen. *Hypertension* **64**, 1131-1140

45.Ren, H., Orozco, I. J., Su, Y., Suyama, S., Gutierrez-Juarez, R., Horvath, T. L., Wardlaw, S. L., Plum, L., Arancio, O., and Accili, D. (2012) FoxO1 target Gpr17 activates AgRP neurons to regulate food intake. *Cell* **149**, 1314-1326

46.Cheng, Z., Guo, S., Copps, K., Dong, X., Kollipara, R., Rodgers, J. T., Depinho, R. A., Puigserver, P., and White, M. F. (2009) Foxo1 integrates insulin signaling with mitochondrial function in the liver. *Nat Med* **15**, 1307-1311

47.Jais, A., Einwallner, E., Sharif, O., Gossens, K., Lu, T. T., Soyal, S. M., Medgyesi, D., Neureiter, D., Paier-Pourani, J., Dalgaard, K., Duvigneau, J. C., Lindroos-Christensen, J., Zapf, T. C., Amann, S., Saluzzo, S., Jantscher, F., Stiedl, P., Todoric, J., Martins, R., Oberkofler, H., Muller, S., Hauser-Kronberger, C., Kenner, L., Casanova, E., Sutterluty-Fall, H., Bilban, M., Miller, K., Kozlov, A. V., Krempler, F., Knapp, S., Lumeng, C. N., Patsch, W., Wagner, O., Pospisilik, J. A., and Esterbauer, H. (2014) Heme oxygenase-1 drives metaflammation and insulin resistance in mouse and man. *Cell* **158**, 25-40

48.Zhang, X., Szeto, C., Gao, E., Tang, M., Jin, J., Fu, Q., Makarewich, C., Ai, X., Li, Y., Tang, A., Wang, J., Gao, H., Wang, F., Ge, X. J., Kunapuli, S. P., Zhou, L., Zeng, C., Xiang, K. Y., and Chen, X. (2013) Cardiotoxic and cardioprotective features of chronic beta-adrenergic signaling. *Circ Res* **112**, 498-509

49.McGuinness, O. P., Shau, V., Benson, E. M., Lewis, M., Snowden, R. T., Greene, J. E., Neal, D. W., and Cherrington, A. D. (1997) Role of epinephrine and norepinephrine in the metabolic response to stress hormone infusion in the conscious dog. *The American journal of physiology* **273**, E674-681

Figure 1. The effect of hepatic Foxo1 deletion on glucagon-induced glucose production and gluconeogenesis. (**A**) Blood glucose level in random-fed mice in 1h after i.p. injection of 0.25 mg/kg body weight glucagon. . Ten-week-old mice per treatment. *n* = 6 mice per group. * P<0.05 vs control mice (CNTR); # P<0.05 for the comparison of designated groups. (**B**) Glucagon tolerance tests for mice after an 18 h overnight fasting. Blood glucose levels (mean ± SEM) were determined at the indicated time points after i.p. injection of 16 μg/kg body weight glucagon. *n* = 6 mice per group, * P<0.05 vs. CNTR. (**C-E**) Quantitative RT-PCR analyses of the livers of mice with i.p. injection of 0.25 mg/kg body glucagon for 1 h. *n*=3 mice per treatment. * P<0.05 vs. CNTR; # P<0.05 for the comparison of designated groups. **(F)** Hepatic glucose production (HGP), glycogenolysis, and gluconeogenesis in primary hepatocytes. Cells were isolated from wild-type (WT) or L-F1KO mice and cultured in DMEM with 2% FBS medium for attachment for 4 h, then switched to HGP buffer with or without pyruvate substrate. HGP were measured 3 h after 100 nM glucagon stimulation and normalized to total protein levels. *n* =3 per group. * P<0.05 vs. CNTR; # P<0.05 vs. L-F1KO.

Figure 2. Regulation of Foxo1 stability and activity by insulin and glucagon in hepatocytes. (**A**) Insulin and glucagon signaling in HepG2 cells. Cells were cultured in DMEM with 10% FBS and then starved in DMEM with 1% BSA medium overnight prior to the treatment of 100 nM insulin or 100 nM glucagon over a 6 h time course. Western-blotting was performed with 150 μg protein of cell lysates to detect total Foxo1, Akt, CREB, pFoxo1-S256, pAkt-T308, and pCREB-S133. (**B-E**) Quantification of total Foxo1/GAPDH (B), p-Foxo1-S256/t-Foxo1 **(C)**, pAKT-T308/Akt **(D)**, and pCREB-S133/CREB **(E)** including from (A) was performed using

Image J. Results are presented as mean ± SEM, * P<0.05 vs. 0 min treatment, *n* = 3 experiments. (**F**)The mRNA expression of *Foxo1* in HepG2 cells. HepG2 cells were cultured in DMEM with 10% FBS and then starved in DMEM with 1% BSA medium overnight prior to the treatment of 100 nM glucagon over a 6 h time course. The Foxo1 mRNA level was detected by qPCR, *n*=3 experiments.

Figure 3. Identification of novel phosphorylation sites of Foxo1 by PKA. (**A**) PKA activates and Akt inhibits Igfbp-1 promoter activity in cells. HepG2 cells were cultured in 6-well plate with DMEM with 10% FBS and then transfected with 0.5 μg Igfbp-1-Luc reporter gene and 0.1 μg RL-luc internal control together with 0.5 μg expression vector for GFP, PKA catalytic subunit, Myr-Akt, HA-Foxo1, or a combination of two as designated. Cell lysates were prepared for luciferase assays, and protein levels of PKA, Akt, Foxo1, or β-actin determined by Western-blotting from 20 μg of total protein. *n*=3 experiments. Values are fold changes of luciferase activity relative to GFP group and presented as mean ± SEM. * P<0.05 vs. GFP; # P<0.05 vs. Foxo1. **(B)** Putative phosphorylation sites of Foxo1 by PKA among different species. **(C)** PKA phosphorylates Foxo1 *in vitro*. 20 μg of recombinant Foxo1-GST was mixed with 5U (0.5 μg) recombinant active PKAc with or without 0.1 mM ATP, for 30 min at 30°C; then the Foxo1-GST and PKAc were resolved in SDS-PAGE after the Coomassie-brilliant blue staining. The intact Foxo1-GST (105 kDa) or cleaved Foxo1 (60 kDa) were incised from the gel and subjected to LC-MS/MS. (**D**) MS/MS spectra of peptide containing S153 and S276 of Foxo1. Antibodies against phosphorylated Foxo1 at S153 and S276 were generated. **(E-F)** Phosphorylation of Foxo1-S276 and S153 by glucagon in cells. (**E**) HepG2 cells were transfected with either scramble siRNA or siRNA-PKACB for 24 h, and then treated with or without 100 nM glucagon

for 60min. Quantification of t-Foxo1, p-Foxo1-S276, p-Foxo1-S153, p-CREB, and CREB was performed using Image J, and normalized by GAPDH. * P<0.05 vs. scramble siRNA; # P<0.05 vs scramble siRNA+glucagon; *n*=3 experiments. (**F**) Primary hepatocytes were cultured and treated with either 100 nM glucagon or 10 μM 8-Br-cAMP for 30 min, or 10 μM PKA inhibitor H89 for 30 min prior to 60 min of 100 nM glucagon treatment. Phosphorylation of Foxo1-S150 and S273 were analyzed by Western-blotting using antibodies at 1:500 dilution. Quantification of p-Foxo1-S273, p-Foxo1-S150, and t-Foxo1 was performed using Image J, and normalized by β-actin. * P<0.05 vs. vehicle; # P<0.05 vs glucagon; *n*=3 experiments.

Figure 4. Glucagon promotes phosphorylation of Foxo1-S153 and S276 *in vivo*. (**A**) Random-fed mice were i.p. injected with glucagon at 0.25 mg/kg body weight, and the liver was collected 15 min after injection to determine hepatic Foxo1 phosphorylation at S150 and S273 by using Western-blotting. Quantification of p-Foxo1-S273, p-Foxo1-S150 was performed using Image J, and normalized by β-actin.* P<0.05 vs. vehicle; # P<0.05 vs glucagon; *n*=4-6 mice per group. (**B-D**) 8-week WT Mice were i.v. injected with GCGR antagonist ([des-His^{1}, Glu^{9}]-Glucagon amide) (1mg/kg body weight) after 6 h fasting, (**B**) blood glucose level was measured at the indicated time points, * P<0.05 vs. vehicle, *n*=4-6 mice per group; (**C**) area under the curve (AUC) from (B) was calculated, * P<0.05 vs. vehicle, *n*=4-6 mice per group; (**D**) liver was collected 45 min after [des-His^{1}, Glu^{9}]-Glucagon amide injection to determine hepatic total Foxo1 and Foxo1 phosphorylation at S150 and S273 by using Western-blotting. Quantification of total Foxo1 and p-Foxo1-S273, p-Foxo1-S150, p-CREB, and CREB was performed using Image J, and normalized by GAPDH.* P<0.05 vs. vehicle, *n*=4-6 mice per group.

Figure 5. Foxo1-S276 phosphorylation controls cAMP-induced Foxo1 nuclear localization in hepatocytes. HepG2 cell were transfected with 5 μg plasmid DNA expressing GFP-Foxo1-WT, S276A, S276D, S153A, or S153D for 18 h, and then treated with/without 10 μM cAMP for 30 min. GFP-positive cells were displayed, DAPI for nucleus stained, and analyzed under confocal microscope. Representative images are shown.

Figure 6. Glucagon or cAMP stimulates Foxo1 nuclear localization and Foxo1-S276 phosphorylation enhancing Foxo1 stability in hepatocytes. (**A**) HepG2 cells were transfected with 5 μg plasmid DNA expressing HA-Foxo1 for 18 h, and then treated with 100 nM glucagon (Glc), 10 μM cAMP or 100 nM insulin for 30 min prior to extraction of nuclear (N) and cytoplasmic proteins (C). 20 μg nuclear protein or 100 μg cytoplasmic protein was immunoblotted to determine the abundance of total Foxo1 in nucleus or cytoplasm. Signal intensity was quantified by image J software for statistical comparison. Cytoplasmic and nuclear protein level were normalized by GAPDH and Histone H1, respectively. *n*=3 experiments. * P<0.05 vs. vehicle in cytoplasm; # P<0.05 vs. vehicle in nucleus. (**B and C**) Distribution of Foxo1-S276 mutant proteins in the nucleus and cytoplasm of cells. HepG2 cells were transfected with 5 μg plasmid DNA expressing Foxo1-WT, S276A, or S276D for 18 h and then treated with/without 100 nM glucagon for 30 min. Nuclear (N) or cytoplasmic protein (C) was extracted to determine protein abundance of Foxo1-S276 mutants in nucleus and cytoplasm. Representative images are shown in (B and C), and Signal intensity was quantified by image J software for statistical comparison. *n*=3 experiments. * P<0.05 vs. vehicle in cytoplasm; # P<0.05 vs. vehicle in nucleus. (**D**) Foxo1-S276 mutations influence Foxo1 stability in a proteasome-dependent manner. Western-blotting was performed to detect total Foxo1 abundance

in HepG2 cells that was transfected with the same amount of plasmid DNA expressing Foxo1-WT, S276A or S276D for 10 h and cells were then starved for 8 h, and treated with 10 μM cycloheximide or 10 μg/ml MG132 for 6 h prior cellular protein collection. Representative images are shown. Signal intensity was quantified and normalized by a-actinin for statistical analysis. * P<0.05 vs. Foxo1-WT; # P<0.05 for the comparison of designated groups. n=3 different experiment. (**E**) Foxo1-S276 mutations influence insulin induced Foxo1 ubiquitination. HepG2 cells were co-transfected with eGFP expression vectors encoding wild-type FoxO1, FoxO1-S276D or FoxO1-S276A and/or FLAG-ubiquitin for 10 h and starve cells for 12 h, and then treated with 100 nM insulin for 12 h. Quantification of t-Foxo1 normalized by α-actinin was performed using Image J. * P<0.05 vs. Foxo1-WT and FLAG-ubiquitin group; # P<0.05 for comparison of designated groups. n=3 different experiment.

Figure 7. Foxo1-S276D impairs insulin-stimulated Foxo1 nuclear export in hepatocytes. (**A**) HepG2 cells were transfected with 5 μg plasmid DNA expressing eGFP-Foxo1-WT or eGFP-Foxo1-S276D for 18 h, and cells were then serum starved for 8 h prior to 100 nM insulin treatment for 0 min, 30 min, 90 min or 120 min. The GFP-positive cells were displayed, DAPI for nucleus stained, and analyzed under the confocal microscope. Representative images are shown. (**B**) HepG2 cells were transfected with 10 μg eGFP expression vectors encoding Foxo1-WT or Foxo1-S276D for 18 h and followed by 8 h serum starvation prior to 100 nM insulin stimulation for 90 min and 120 min. Western-blotting was performed for total Foxo1 and phospho-Foxo1-S256 in cytoplasm and nucleus. (**C**) Quantification of total Foxo1 and pFoxo1-S256/t-Foxo1 was performed by image J. Cytoplasmic and nuclear protein level were normalized by GAPDH and Histone H1, respectively. Results are presented as mean ± SEM, *n*=3 different

experiments. * P<0.05 vs. 0 min of insulin treatment from Foxo1-WT in cytoplasm; # P<0.05 vs. 0 min of insulin treatment from Foxo1-WT in nucleus.

Figure 8. Foxo1-S273 mutations impair blood glucose and hepatic glucose production in mice. (**A**) Blood glucose levels of random-fed or 18 h fasted mice. *n* = 4-6 mice per genotype. * P<0.05 vs. WT mice. (**B**) Quantitative PCR analysis of expression of Igfbp-1 and G6pc in the liver of 18h fasted mice, n=4 mice per genotype, * P<0.05 vs. WT mice. (**C**) Foxo1 protein levels in the livers of the mutant mice. Western-blotting results from two mice per genotype are shown representatively. * P<0.05, ** P<0.01 vs. WT. *n*=4 per group. (**D**) HGP assays in the primary hepatocytes isolated from WT, Foxo1-S273$^{A/A}$, and Foxo1-S273$^{D/D}$ knock-in mice. Fresh hepatocytes were isolated from these mice and HGP were measured 3 h after 100 nM glucagon stimulation and normalized to total protein levels. *n*= 3 per treatment. * P<0.05 vs WT with vehicle group. # P<0.05 for the comparison of designated groups. (**E-F**) Glucagon tolerance test, (**E**) Glucagon tolerance tests for mice after an 18 h overnight fasting. Blood glucose levels (mean ± SEM) were determined at the indicated time points after i.p. injection of 16 μg/kg body weight glucagon. *n* = 6 mice, * P<0.05 vs. WT; (**F**) Area under the curve (AUC) from (E) was calculated. * P<0.05 vs. WT, *n*=4-6 per group. (**G**) Blood glucagon, insulin and glucose levels in WT and db/db mice in an 18 h fasting state. * P<0.05 vs. WT, n=4 mice per group. (**H**) pFoxo1-S273, pFoxo1-S253, total Foxo1, pPKA-T179, PKA, histone H1, and GAPDH in 100 μg cytoplasmic protein (C) and 20 μg nuclear proteins (N) of mouse livers were determined by Western-blotting. (**I**) Quantification of pFoxo1-S273, p-S253, total Foxo1, pPKA-T197, or PKA was performed by image J. The cytoplasmic and nuclear protein level were normalized by GAPDH and Histone H1, respectively. * P<0.05 vs. WT, n=3 mice per group. Results are shown

as mean ± SEM. (**J**) Blood glucagon, insulin and glucose levels in LFD- and HFD-fed WT mice in an 18 h fasting state. * P<0.05 vs. LFD, n=4 mice per group. (**K**) pFoxo1-S273, total Foxo1, pCREB, and CREB level of mouse livers were determined by Western-blotting. (**L)** Quantification of pFoxo1-S273, total Foxo1, pCREB, and CREB was performed by image J.. * P<0.05 vs. LFD, n=4 mice per group. Results are shown as mean ± SEM.

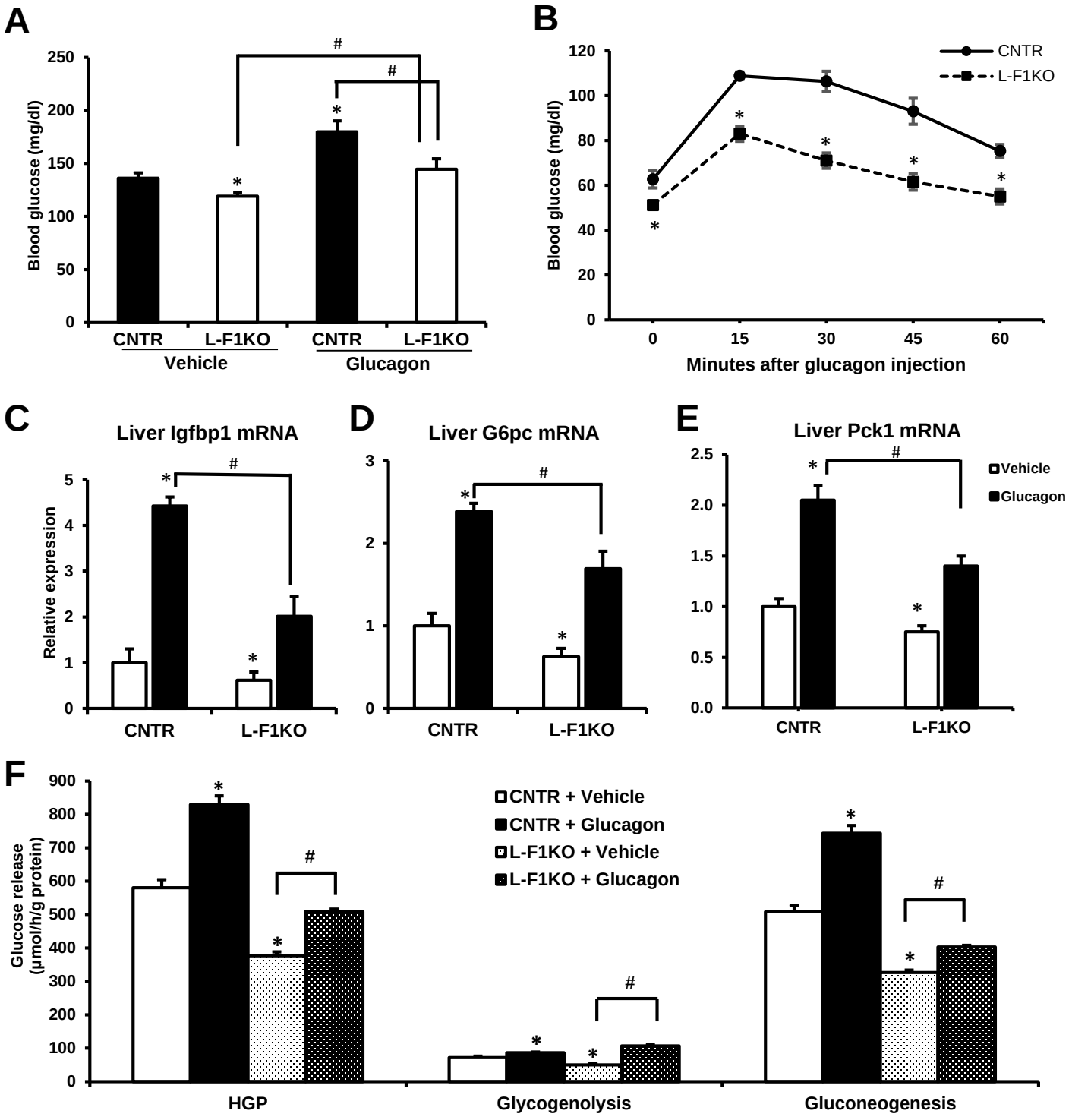
A
Blood glucose (mg/dl)
250
200
150
100
50
0
#
#
*
*
*
CNTR
L-F1KO
CNTR
L-F1KO
Vehicle
Glucagon
B
Blood glucose (mg/dl)
120
100
80
60
40
20
0
CNTR
L-F1KO
*
*
*
*
*
0
15
30
45
60
Minutes after glucagon injection
C
Liver Igfbp1 mRNA
Relative expression
5
4
3
2
1
0
#
*
*
CNTR
L-F1KO
D
Liver G6pc mRNA
3
2
1
0
#
*
*
CNTR
L-F1KO
E
Liver Pck1 mRNA
2.5
2.0
1.5
1.0
0.5
0.0
#
*
*
Vehicle
Glucagon
CNTR
L-F1KO
F
Glucose release
(µmol/h/g protein)
900
800
700
600
500
400
300
200
100
0
*
*
*
*
*
*
#
#
#
CNTR + Vehicle
CNTR + Glucagon
L-F1KO + Vehicle
L-F1KO + Glucagon
HGP
Glycogenolysis
Gluconeogenesis

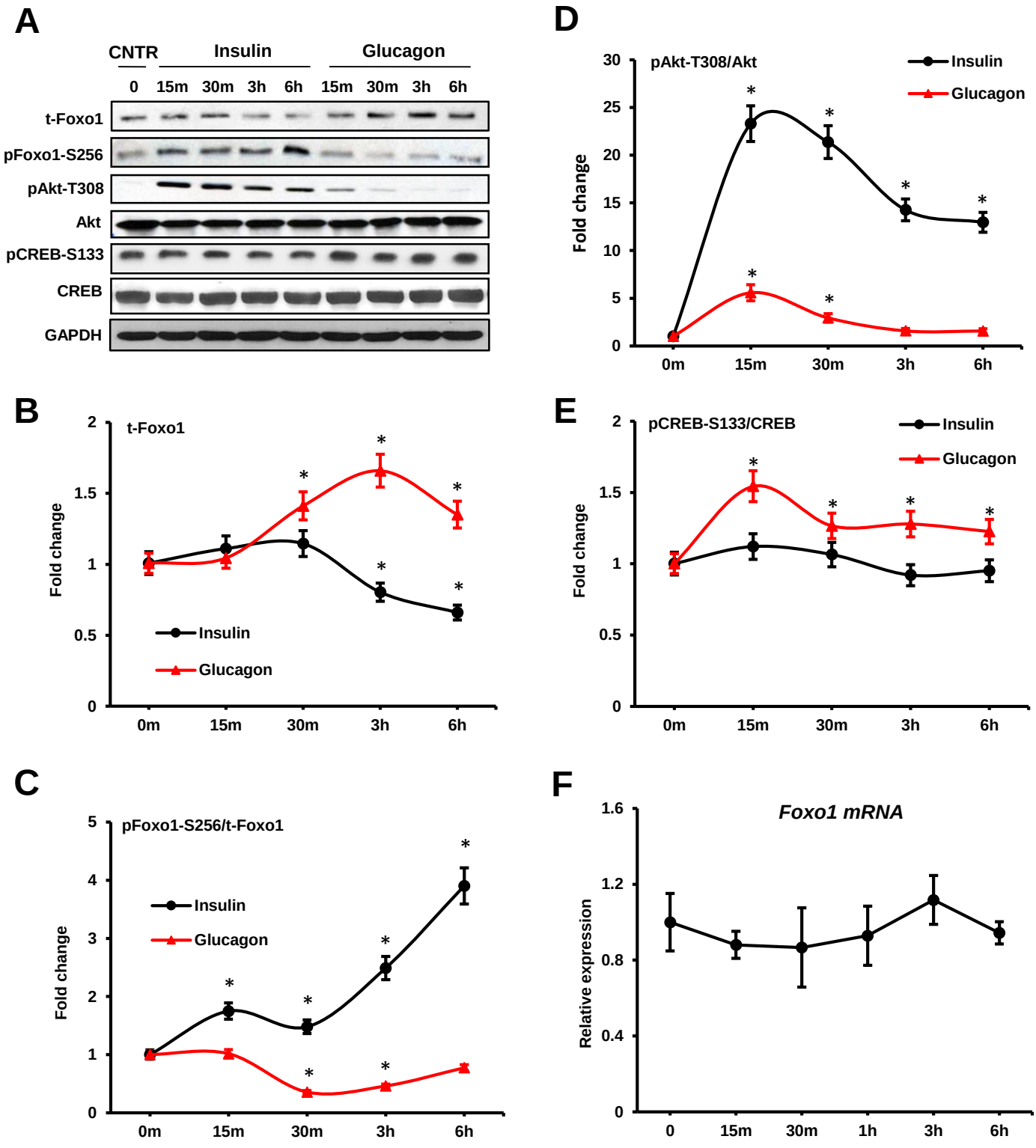
A
CNTR
Insulin
Glucagon
0
15m
30m
3h
6h
15m
30m
3h
6h
t-Foxo1
pFoxo1-S256
pAkt-T308
Akt
pCREB-S133
CREB
GAPDH
B
t-Foxo1
Fold change
Insulin
Glucagon
0m
15m
30m
3h
6h
C
pFoxo1-S256/t-Foxo1
Fold change
Insulin
Glucagon
D
pAkt-T308/Akt
Fold change
Insulin
Glucagon
E
pCREB-S133/CREB
Fold change
Insulin
Glucagon
F
Foxo1 mRNA
Relative expression
0
15m
30m
1h
3h
6h

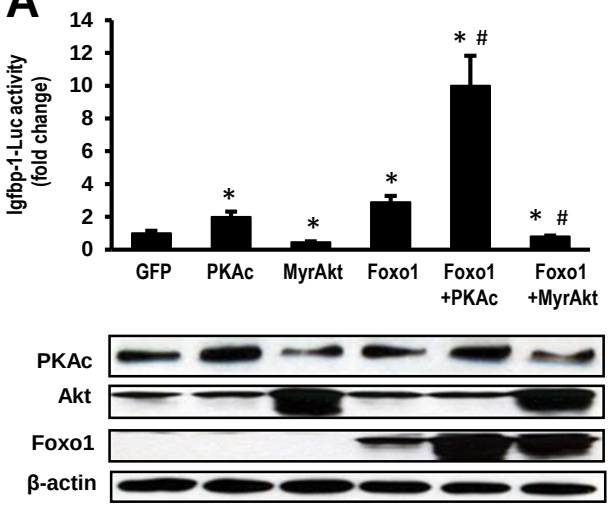
A
Igfbp-1-Luc activity (fold change)
GFP
PKAc
MyrAkt
Foxo1
Foxo1 +PKAc
Foxo1 +MyrAkt
PKAc
Akt
Foxo1
β-actin

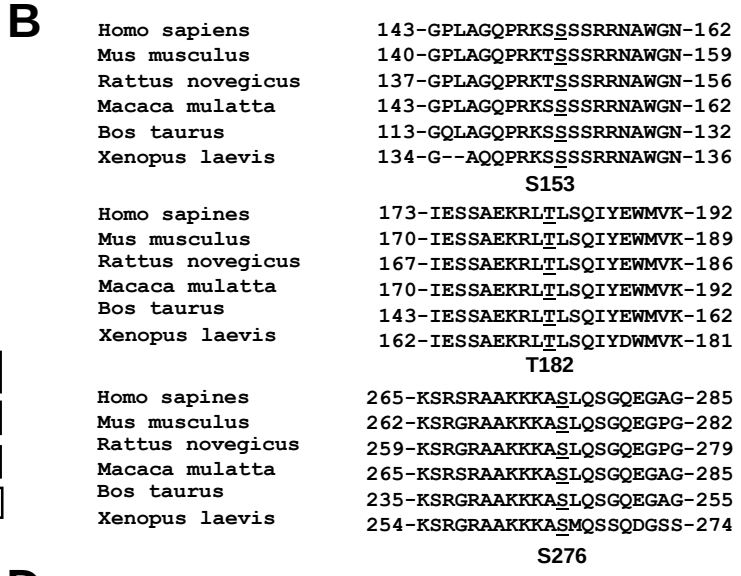
B
Homo sapiens 143-GPLAGQPRKSSSSRRNAWGN-162
Mus musculus 140-GPLAGQPRKTSSSRRNAWGN-159
Rattus novegicus 137-GPLAGQPRKTSSSRRNAWGN-156
Macaca mulatta 143-GPLAGQPRKSSSSRRNAWGN-162
Bos taurus 113-GQLAGQPRKSSSSRRNAWGN-132
Xenopus laevis 134-G--AQQPRKSSSSRRNAWGN-136
S153
Homo sapines 173-IESSAEKRLTLSQIYEWMVK-192
Mus musculus 170-IESSAEKRLTLSQIYEWMVK-189
Rattus novegicus 167-IESSAEKRLTLSQIYEWMVK-186
Macaca mulatta 170-IESSAEKRLTLSQIYEWMVK-192
Bos taurus 143-IESSAEKRLTLSQIYEWMVK-162
Xenopus laevis 162-IESSAEKRLTLSQIYDWMVK-181
T182
Homo sapines 265-KSRSRAAKKKASLQSGQEGAG-285
Mus musculus 262-KSRGRAAKKKASLQSGQEGPG-282
Rattus novegicus 259-KSRGRAAKKKASLQSGQEGPG-279
Macaca mulatta 265-KSRSRAAKKKASLQSGQEGAG-285
Bos taurus 235-KSRGRAAKKKASLQSGQEGAG-255
Xenopus laevis 254-KSRGRAAKKKASMQSSQDGSS-274
S276

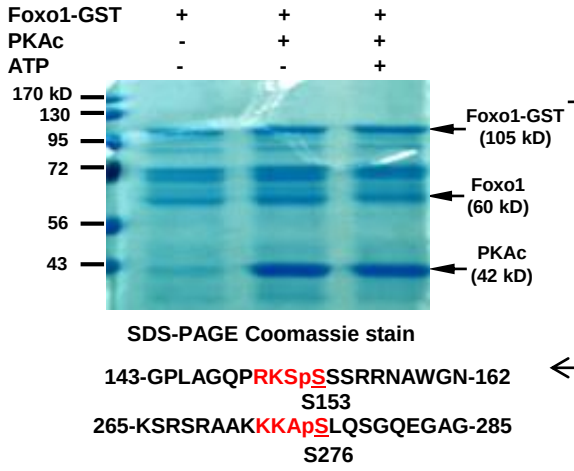
C
Foxo1-GST + + +
PKAc - + +
ATP - - +
170 kD
130
95
72
56
43
Foxo1-GST (105 kD)
Foxo1 (60 kD)
PKAc (42 kD)
SDS-PAGE Coomassie stain
143-GPLAGQPRKSpSSSRRNAWGN-162
S153
265-KSRSRAAKKKApSLQSGQEGAG-285
S276

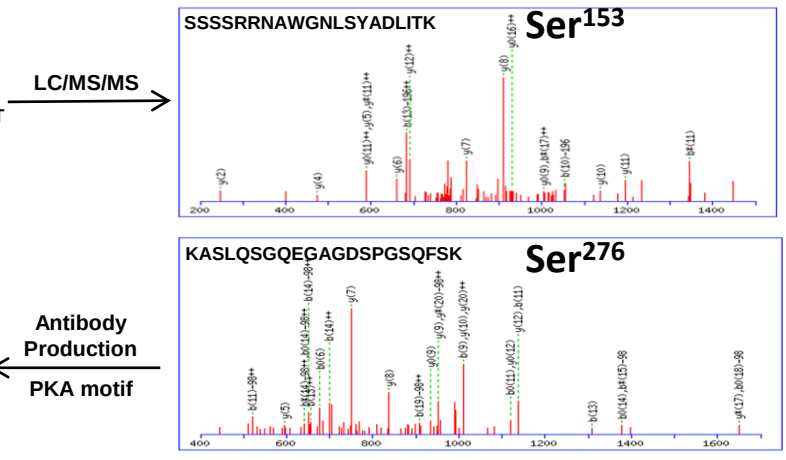
D
LC/MS/MS
SSSSRRNAWGNLSYADLITK
Ser153
KASLQSGQEGAGDSPGSQFSK
Ser276
Antibody Production
PKA motif

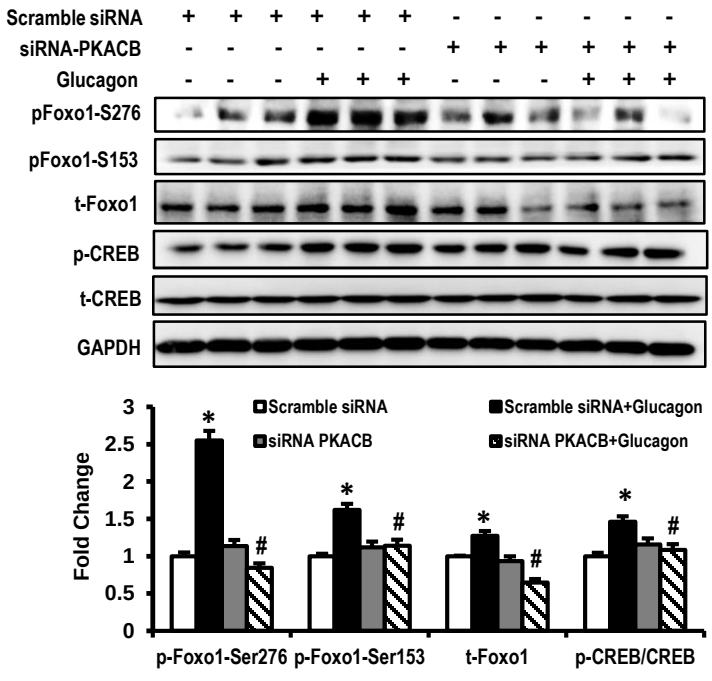
E
Scramble siRNA + + + + + + - - - - - -
siRNA-PKACB - - - - - - + + + + + +
Glucagon - - - + + + - - - + + +
pFoxo1-S276
pFoxo1-S153
t-Foxo1
p-CREB
t-CREB
GAPDH
Scramble siRNA
siRNA PKACB
Scramble siRNA+Glucagon
siRNA PKACB+Glucagon
Fold Change
p-Foxo1-Ser276
p-Foxo1-Ser153
t-Foxo1
p-CREB/CREB

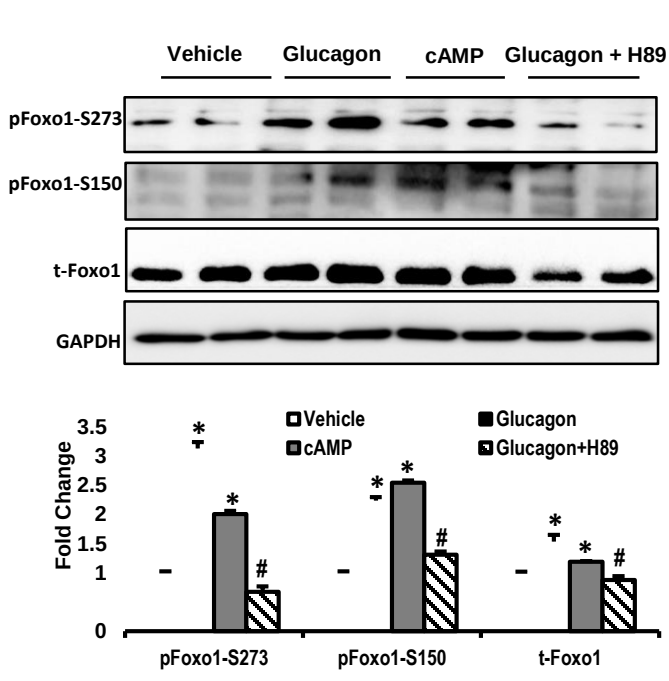
F
Vehicle
Glucagon
cAMP
Glucagon + H89
pFoxo1-S273
pFoxo1-S150
t-Foxo1
GAPDH
Vehicle
cAMP
Glucagon
Glucagon+H89
Fold Change
pFoxo1-S273
pFoxo1-S150
t-Foxo1

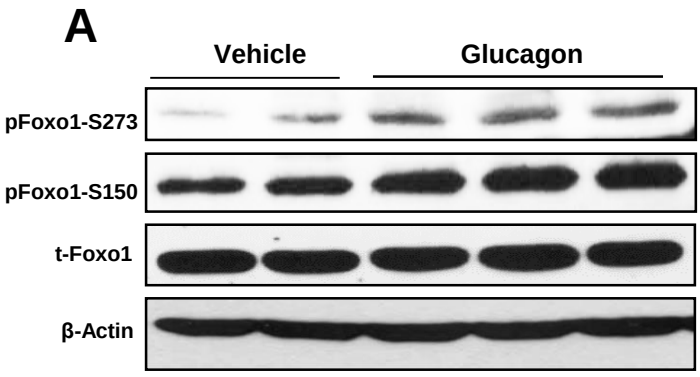
A
Vehicle
Glucagon
pFoxo1-S273
pFoxo1-S150
t-Foxo1
β-Actin

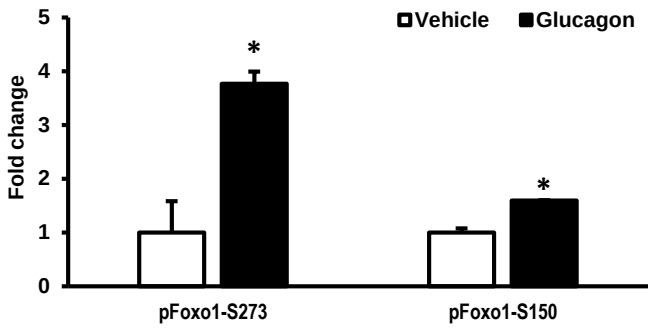
Vehicle
Glucagon
Fold change
5
4
3
2
1
0
*
*
pFoxo1-S273
pFoxo1-S150

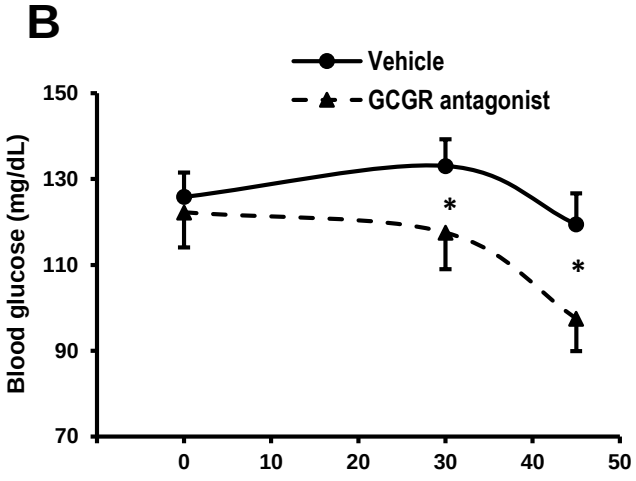
B
Vehicle
GCGR antagonist
Blood glucose (mg/dL)
150
130
110
90
70
0
10
20
30
40
50
*
*

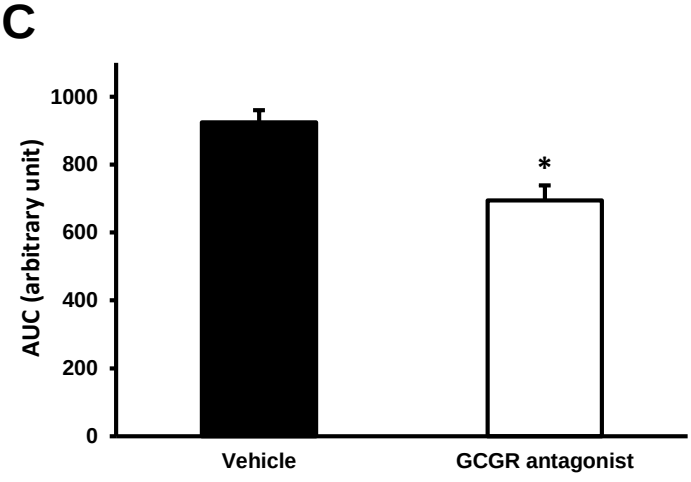
C
AUC (arbitrary unit)
1000
800
600
400
200
0
*
Vehicle
GCGR antagonist

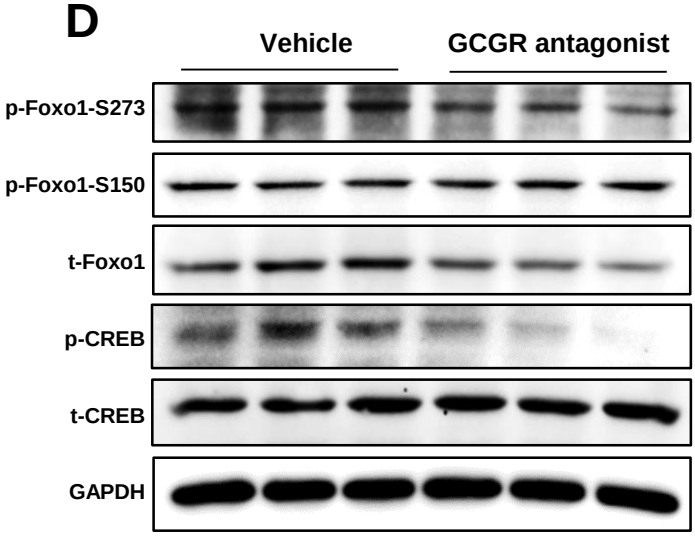
D
Vehicle
GCGR antagonist
p-Foxo1-S273
p-Foxo1-S150
t-Foxo1
p-CREB
t-CREB
GAPDH

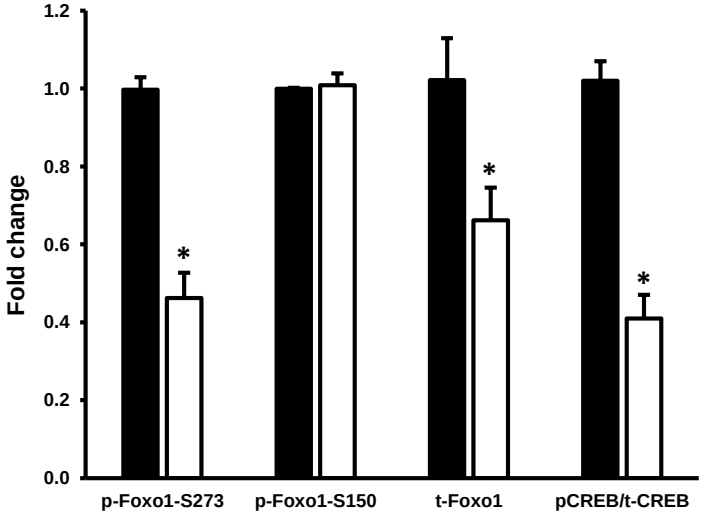
Fold change
1.2
1.0
0.8
0.6
0.4
0.2
0.0
*
*
*
p-Foxo1-S273
p-Foxo1-S150
t-Foxo1
pCREB/t-CREB

Figure 5

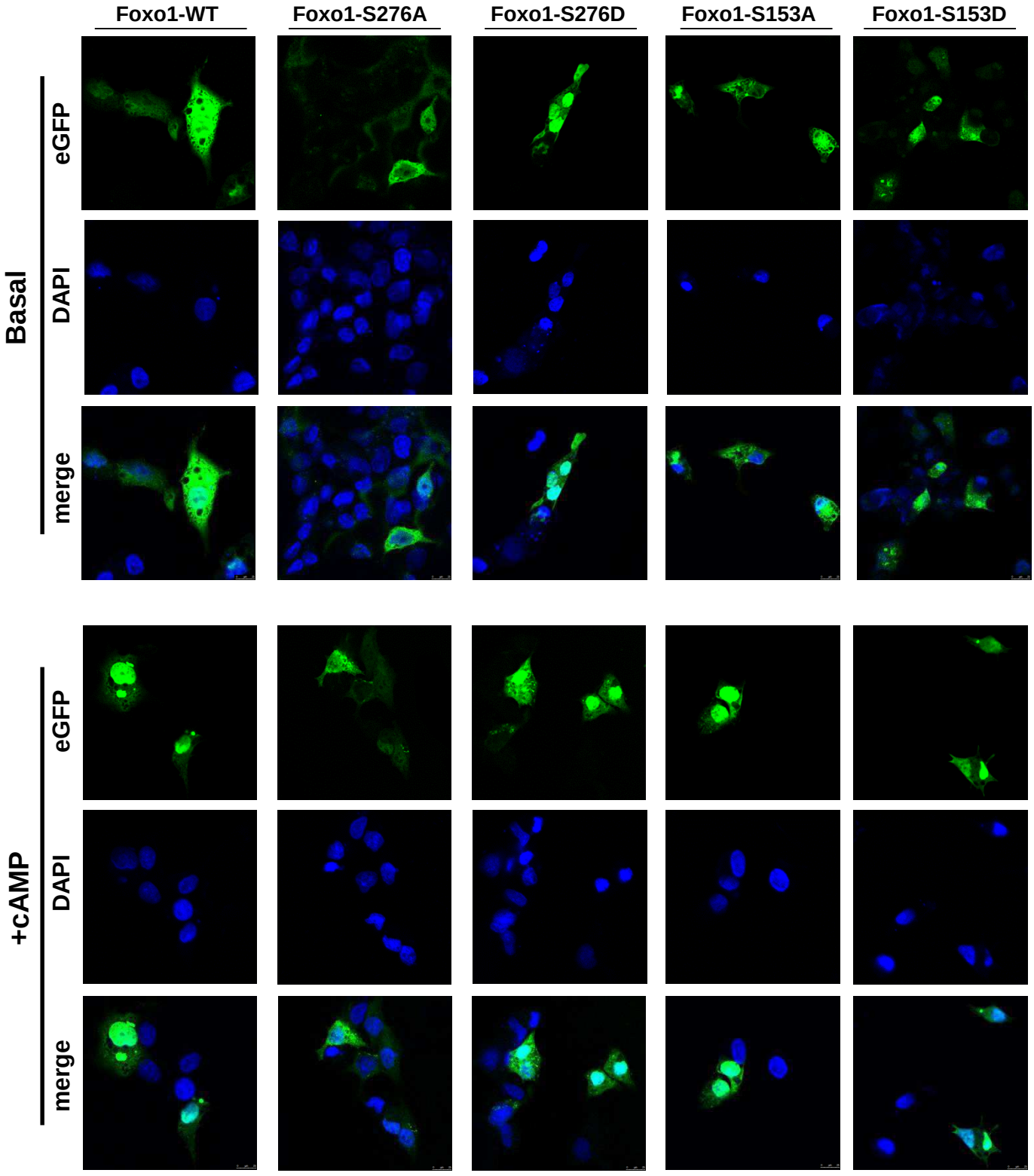
Foxo1-WT
Foxo1-S276A
Foxo1-S276D
Foxo1-S153A
Foxo1-S153D
Basal
+cAMP
eGFP
DAPI
merge

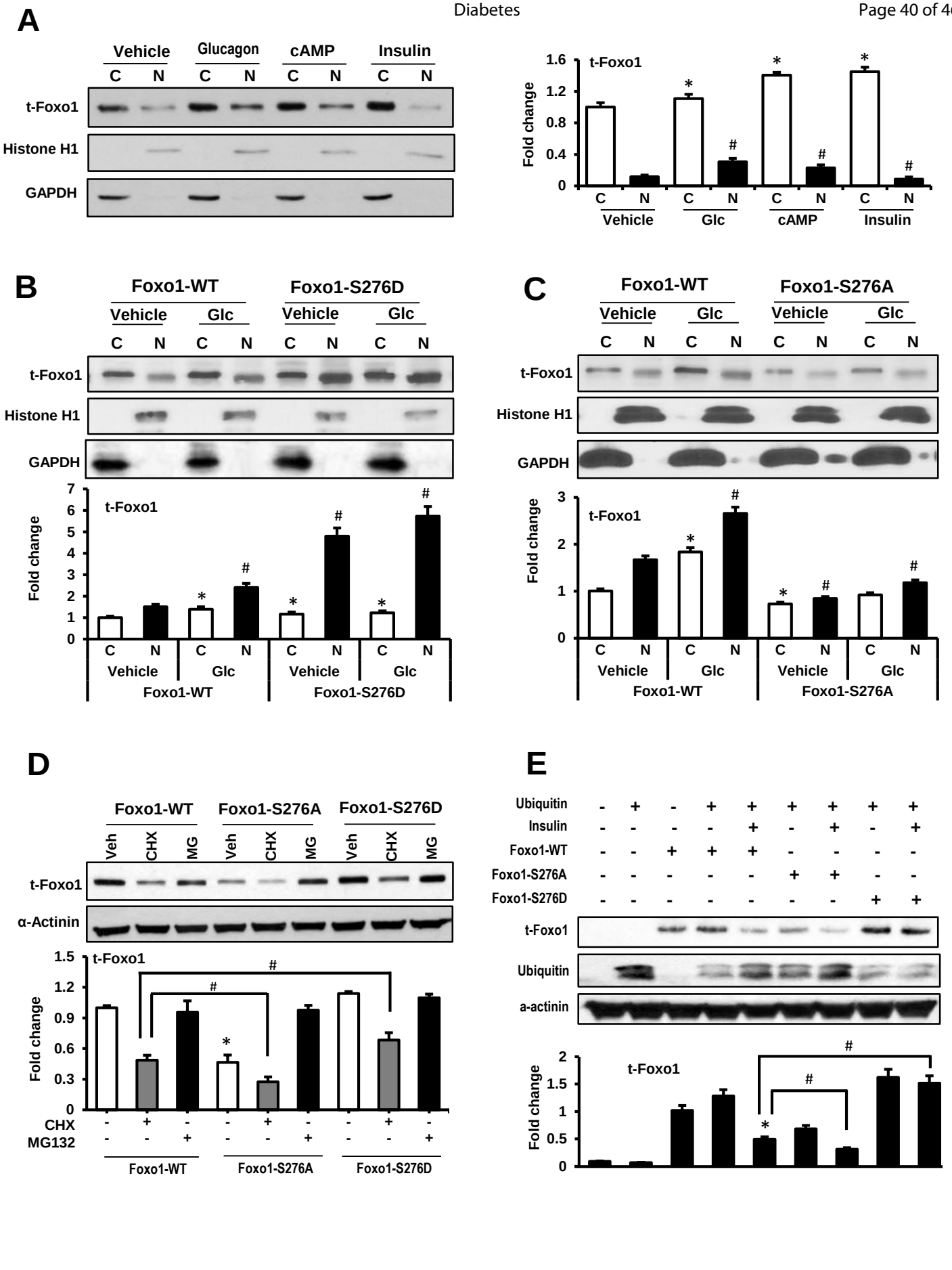
A
Vehicle
Glucagon
cAMP
Insulin
C N C N C N C N
t-Foxo1
Histone H1
GAPDH
t-Foxo1
Fold change
Vehicle
Glc
cAMP
Insulin
B
Foxo1-WT
Foxo1-S276D
Vehicle
Glc
t-Foxo1
Histone H1
GAPDH
Foxo1-WT
Foxo1-S276D
C
Foxo1-WT
Foxo1-S276A
Foxo1-S276A
D
Foxo1-WT
Foxo1-S276A
Foxo1-S276D
Veh
CHX
MG
t-Foxo1
α-Actinin
CHX
MG132
E
Ubiquitin
Insulin
Foxo1-WT
Foxo1-S276A
Foxo1-S276D
t-Foxo1
Ubiquitin
a-actinin

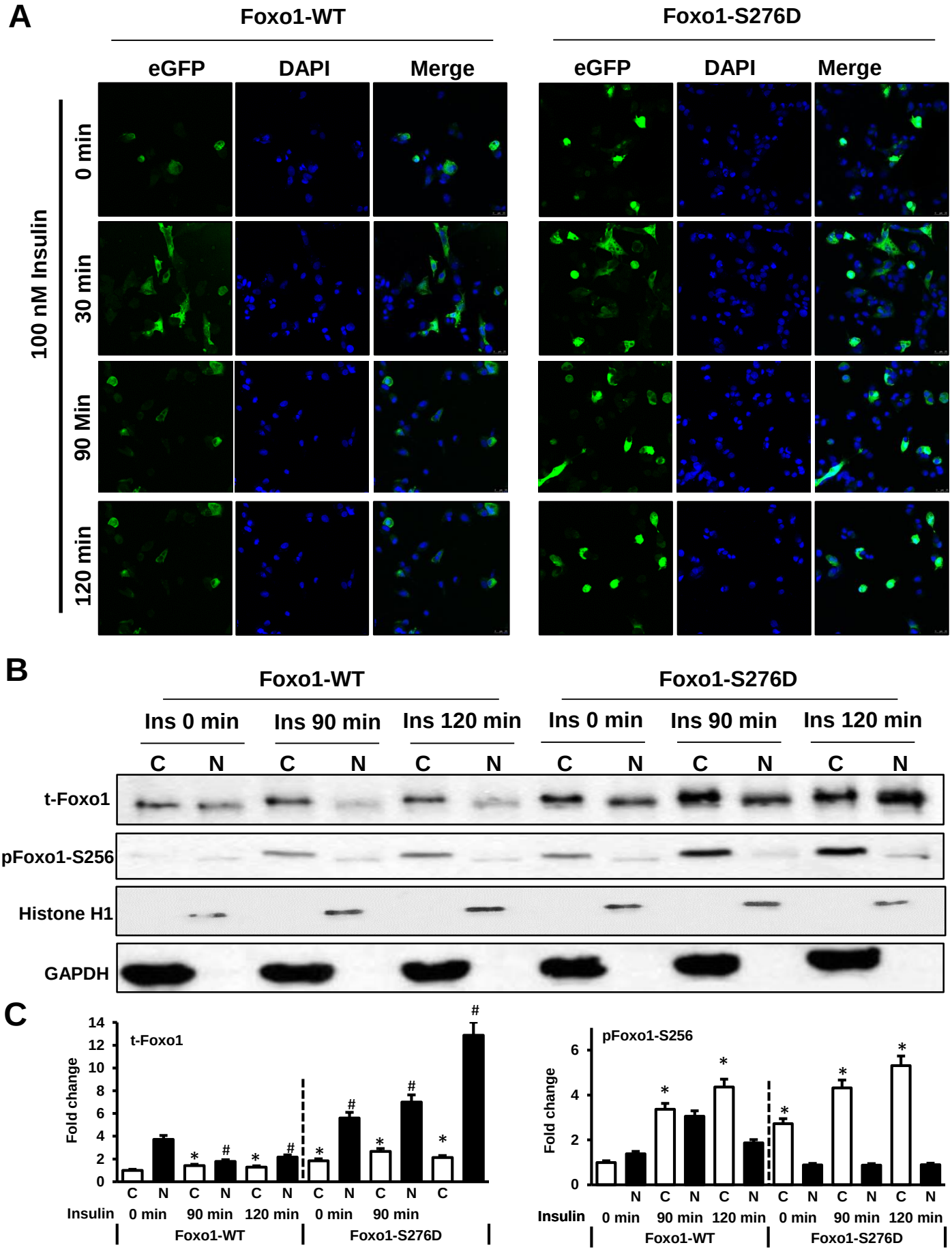
A
Foxo1-WT
Foxo1-S276D
eGFP
DAPI
Merge
100 nM Insulin
0 min
30 min
90 Min
120 min
B
Foxo1-WT
Foxo1-S276D
Ins 0 min
Ins 90 min
Ins 120 min
C
N
t-Foxo1
pFoxo1-S256
Histone H1
GAPDH
C
t-Foxo1
Fold change
Insulin
0 min
90 min
120 min
Foxo1-WT
Foxo1-S276D
pFoxo1-S256

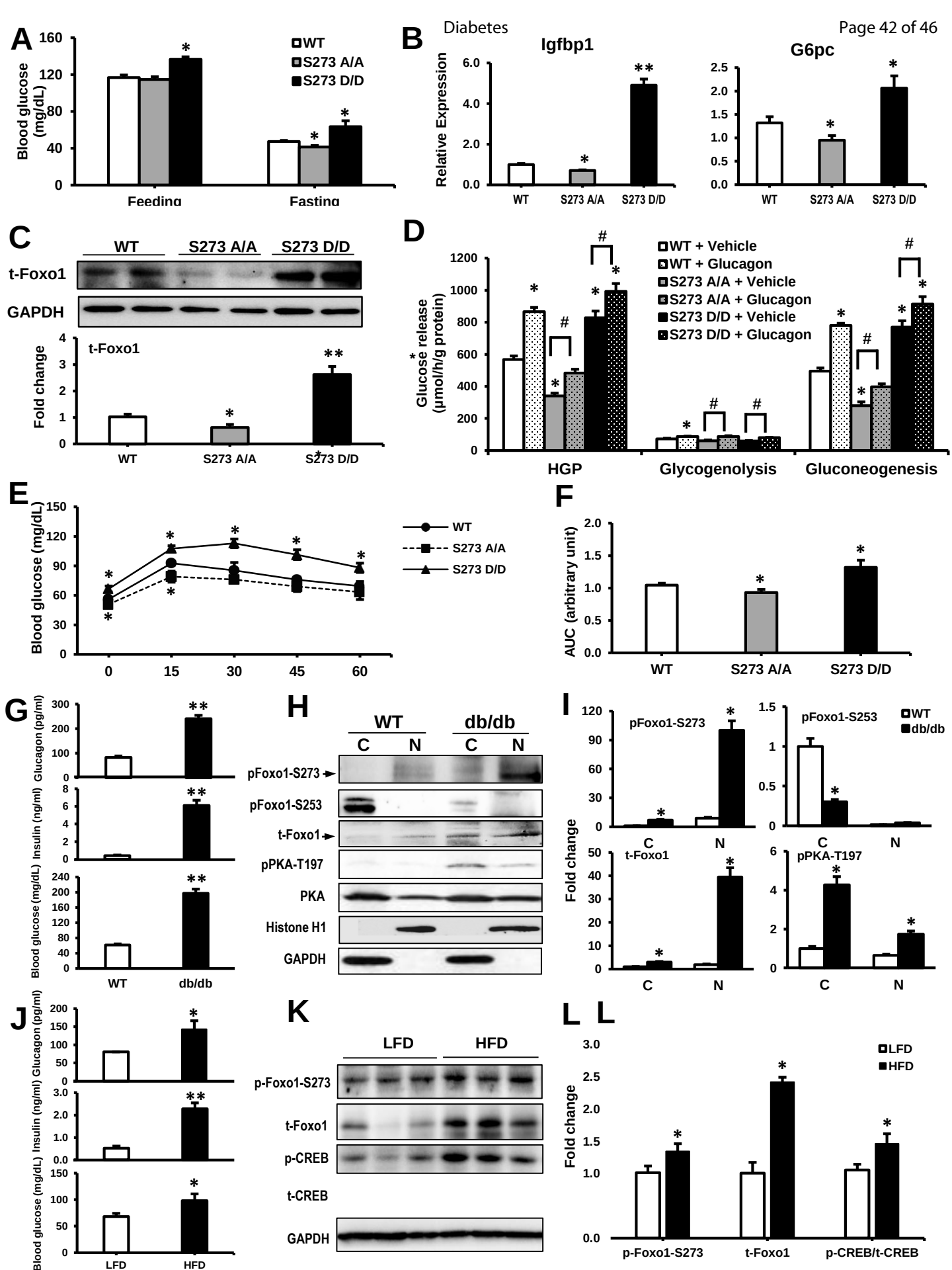
A
Blood glucose (mg/dL)
WT
S273 A/A
S273 D/D
Feeding
Fasting
B
Igfbp1
G6pc
Relative Expression
WT
S273 A/A
S273 D/D
C
WT
S273 A/A
S273 D/D
t-Foxo1
GAPDH
Fold change
D
Glucose release (μmol/h/g protein)
WT + Vehicle
WT + Glucagon
S273 A/A + Vehicle
S273 A/A + Glucagon
S273 D/D + Vehicle
S273 D/D + Glucagon
HGP
Glycogenolysis
Gluconeogenesis
E
Blood glucose (mg/dL)
WT
S273 A/A
S273 D/D
F
AUC (arbitrary unit)
G
Glucagon (pg/ml)
Insulin (ng/ml)
Blood glucose (mg/dL)
WT
db/db
H
WT
db/db
C
N
pFoxo1-S273
pFoxo1-S253
t-Foxo1
pPKA-T197
PKA
Histone H1
GAPDH
I
pFoxo1-S273
pFoxo1-S253
t-Foxo1
pPKA-T197
Fold change
WT
db/db
J
Glucagon (pg/ml)
Insulin (ng/ml)
Blood glucose (mg/dL)
LFD
HFD
K
LFD
HFD
p-Foxo1-S273
t-Foxo1
p-CREB
t-CREB
GAPDH
L
Fold change
LFD
HFD
p-Foxo1-S273
t-Foxo1
p-CREB/t-CREB

SUPPLEMENTAL MATERIAL

Liquid Chromatography-mass spectrometry (LC-MS). To identify the phosphorylation sites of Foxo1, we performed LC-MS/MS analysis. The specific bands on the SDS-PAGE gel after Coomassie-brilliant blue staining were excised, cut into several pieces, and subjected to dimethyl formamide (DMF)-assisted trypsin digestion. The digested peptides were analyzed by LC-MS/MS. Briefly, the pieces of the gel was dissolved in 50 mM NH_4HCO_3 buffer (pH8.0) containing 40% DMF and added with 20 µl of 2 µg trypsin, and incubated overnight at 37 °C. After digestion, the solution was further diluted by adding three-fold volume of deionized water. After centrifugation, the supernatant was collected. The debris were washed in 80 µL of 70% acetonitrile and 1% rifluoroacetic acid with sonication for 30 min and then centrifuged. Both supernatants were combined and concentrated in a Speed-Vac and stored at -20 °C until further use. To identify the unknown proteins and phosphorylation sites (p-sites), HPLC conjugated electrospray ionization (ESI) ion trap mass spectrometry were employed. The samples were separated on an Alltech Vydac MS C18 column (300 A, 5µm, 100 mm × 300 µm) at a flow rate of 5µl/min using a mobile phase of (A) 0.1% v/v formic acid in water and (B) 0.1% v/v formic acid in acetonitrile. The chromatography system was directly coupled to an ESI Ion-trap mass spectrometer. Raw spectrum data were processed and MASCOT-compatible mgf files were created using DataAnalysis software (Bruker Daltonics). Peptide searching and analysis were performed using MASCOT software (Matrixscience, London, UK). The NCBI gene bank database was used for protein identification.

Generation of phosphospecific antibodies for Foxo1. The conjugated peptides were used to immunize rabbits. Six weeks later serum was collected and passed through a CH-sepharose column containing beads coupled to dephospho-peptide antigen, followed by affinity chromatography on the column with beads covalently coupled to phosphor-peptide antigen. Phosphospecific antibodies were eluted with 0.1 M glycine, pH 2.4, immediately adjusted to pH 8.0 with Tris-base and stored at -20ºC. The phosphospecific antibodies was passed quality control tests, in which 50% titer Elisa test was used to determine signal intensity. The reference of 153,000 for antibody against pFoxo1-S276 and 105,000 for antibody against pFoxo1-S153 achieved, indicative for high specificity signals to corresponding specific phosphorylation sites, in comparison with control non-phosphorylated peptides as reference of signal less than 100 .

Chemicals. Insulin, 8-Br-cAMP, glucagon, [des-His^1, Glu^9]-Glucagon amide, MG132, and CHX were purchased from Sigma; Foxo1, pFoxo1-S256, Akt, pAkt-T308, PKA, pPKA-T197, and β-actin antibodies were from Cell Signaling Technology. Antibodies specific for CREB, pCREB-S133, Histone H1, and β-actin were from Santa Cruz. The scramble siRNA (AM4611) and siRNA-PKACB (4390824) were purchased from Thermo Fisher (Waltham, MA).

PKA knock-down assay. HepG2 cells were cultured with DMEM with 10% FBS for 6 h. Cell culture were then subjected to Lipofectamine® 3000 (Life technologies) with scramble siRNA or siRNA-PKACB according to manufacturer's instruction. 24 h after transfection, cells were subjected to further treatment.

Generation of Foxo1-S273A and Foxo1-S273D Knock-in mice. Mouse Foxo1 gene (Ensembl: ENSMUSG00000044167) is located on mouse chromosome 3. Three exons

have been identified, with the ATG start codon in exon 1 and TAA stop codon in exon 2. The Foxo1-S273 is located in exon 2 and selected as target sites. The gRNA was designed and the targeting vectors constructed, and oligo donors with targeting sequence flanked by 60bp homologous sequences were designed. The S273A (TCT to GCT), S273D (TCT to GAT) mutation site in the donor oligo was introduced into exon 2 by homology-directed repair. The Cas9 mRNA and gRNA were generated by *in vitro* transcription and oligo donor was co-injected into fertilized eggs for the KI mouse production.

Figure S1

A

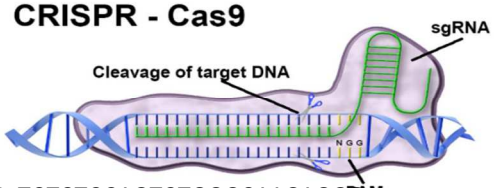

gRNA2: TCTCTCCAGTCTGGGCAAGAGGG

Oligo 1 A mutation

TCCATGGACAACAACAGTAAATTTGCTAAGAGCCGAGG
GCGGGCTGCTAAGAAAAAAGCAGCTCTtCAGTCTGGG
CAAGAGGGTCCTGGAGACAGCCCTGGGTCTCAGTTTT
CTAAGTGGCCTGCG

Oligo 2 D mutation

TCCATGGACAACAACAGTAAATTTGCTAAGAGCCGAGG
GCGGGCTGCTAAGAAAAAAGCAGATCTtCAGTCTGGGC
AAGAGGGTCCTGGAGACAGCCCTGGGTCTCAGTTTTC
TAAGTGGCCTGCG

B

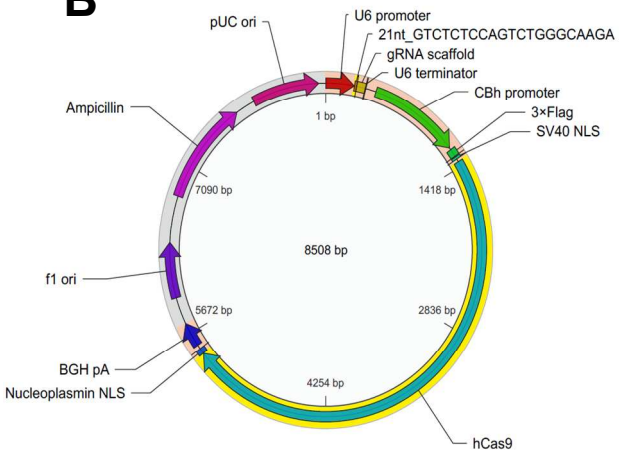

C

DNA Sequencing Primer (Forward Sequencing): 5'-

Specific primers: mFoxo1-gRNA-SPF:

GGGGGAGTGCTGCACTTCTAACATA

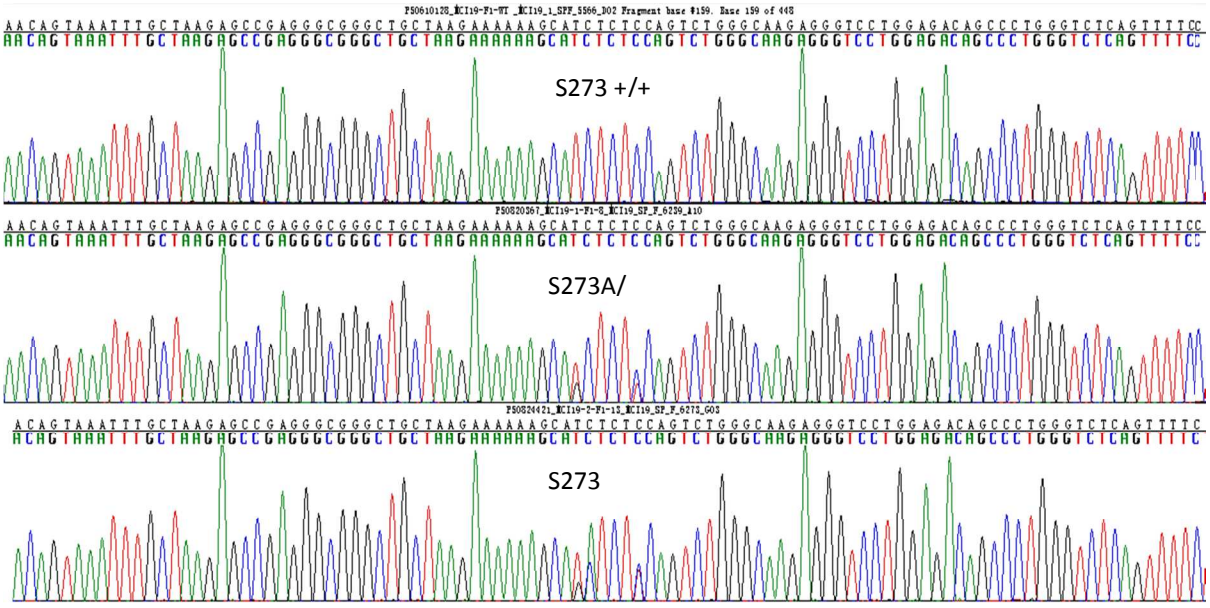

D

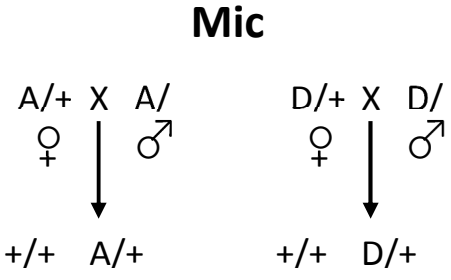

Figure S1. DNA sequencing of Foxo1-S273A and Foxo1-S273D heterozygotes and homozygotes in mice. (**A**) Construction of plasmid DNA expressing Foxo1 guidance RNA with human Cas9 expression vector. (**B**) Sequencing results of Foxo1 alleles from +/+ (wild-type or WT), A/+, and D/+ heterozygous founder mice. (**C**) The breeding strategy and genotyping for Foxo1-S273$^{+/+}$, S273$^{A/A}$, and S273$^{D/D}$ alleles in mice.